on EMCV-infected mice and to characterize the infiltrating cells, which possibly produce TNF-α, into the heart in this model.

## Results

**Survival of mice after LPS stimulation during EMCV infection.** The mice were intraperitoneally inoculated with 20 pfu of EMCV and were intravenously injected with 10 μg LPS at 0, 2, and 5 days after the EMCV inoculation. At 5 days after EMCV infection, all mice died after LPS treatment within 24 h, but the mice subjected to this treatment at 0 and 2 days after EMCV infection were alive (Table 1). Moreover, at 5 days after EMCV infection, LPS-induced lethal shock developed in the mice in an LPS dose-dependent manner (Table 2).

To compare the survival rate between WT and TNF-α KO mice after LPS treatment during EMCV infection, the mice were treated intravenously with 10 μg LPS at 5 days after EMCV infection. All WT mice died after LPS treatment within 24 h at 5 days after EMCV infection, whereas TNF-α KO mice did not die. Moreover, LPS-induced lethality in WT mice was improved by anti-TNF-α antibody (100 μg/mouse) treatment before LPS stimulation (Table 3).

**Effect of EMCV infection on LPS-induced TNF-α production.** The concentration of serum TNF-α was measured at 0, 2, and 8 h after LPS treatment in each EMCV infection period. LPS-induced TNF-α concentration in the serum was markedly increased at 5 days after EMCV infection than at 0 and 2 days after EMCV infection (Fig. 1A).

For the localization of TNF-α production, TNF-α mRNA expression was determined in the brain, heart, liver, lung, and spleen at 0, 1, and 8 h after LPS treatment. TNF-α mRNA expression in the brain, heart, and liver of mice was significantly increased at 5 days after EMCV infection as compared with that at 0 and 2 days after EMCV infection (Fig. 1B).

**Histopathological finding and viral load of the tissues after EMCV infection.** Histological changes were observed in the brain and heart. The mice were inoculated intraperitoneally with 20 pfu of EMCV. Neuronal cell death and the presence of some inflammatory cells in hippocampus or brain surface of the brain and marked infiltration of inflammatory cells in the heart were seen at 5 days after EMCV infection. The infiltrating cells mainly included macrophages and neutrophils (Fig. 2A). In the liver, a little infiltration of inflammatory cells was observed at 5 days after EMCV infection, and no remarkable change was seen in the lung during each infection period (Data not shown). All tissues at 8 h after LPS treatment in EMCV-infected mice were not observed the significant increase of inflammatory cells in comparison with the tissues before LPS treatment (data not shown).

We measured the viral load in the brain, heart, liver, lung and spleen at 2 and 5 days after EMCV infection. Viral loads in all tissues at 5 days after EMCV infection were increased as compared with those at 2 days after EMCV infection. In particular, viral loads in the brain and heart markedly increased at 5 days after the infection (Fig. 2B).

**Effect of EMCV infection on mRNA expression of chemokines in the tissues.** Chemoattractant protein-1 (MCP-1) is a major chemoattractant responsible for the recruitment of macrophages[19,20]. macrophage inflammatory protein-2 (MIP-2) and keratinocyte-derived chemokine (KC), which are produced by macrophages, exhibit potent neutrophil chemotactic activity[21,22]. Because the infiltrated cells were mainly composed of macrophages and neutrophils as revealed by histopathological findings (Fig. 2A), the mRNA expressions of MCP-1, MIP-2, and KC were determined in the brain and heart at 0, 2, and 5 days after EMCV infection. The mRNA expression of these chemokines in the brain and heart on 5 days after EMCV infection was significantly up-regulated as compared with that at 0 and 2 days after EMCV infection (Fig. 3). MCP-1 mRNA expression at 5 days after EMCV infection was 808-fold in the brain and 125-fold in the heart based on 0 days. Similarly, MIP-2 mRNA expression was enhanced 254-fold in the brain and 44-fold in the heart, and KC mRNA expression was increased 23-fold in the brain and also in the heart. Although the expression of chemokines in the liver, lung and spleen had a tendency to up-regulated at 5 days after EMCV infection, the up-regulation was not more remarkable than that in the brain or heart.

**Effect of EMCV infection on TLR4 mRNA expression in tissues and infiltrating cells in the heart.** The expression of TLR4 mRNA was examined in the brain, heart, liver, lung and spleen at 0, 2, and 5 days after EMCV infection. TLR4 mRNA expression in the brain, heart, and liver at 5 days after EMCV infection was significantly increased. On the other hand, TLR4 mRNA expression in the lung and spleen showed no significant change after viral infection (Fig. 4A).

Next, we determined the phenotype of mononuclear cells (MNCs) from the heart at 5 days after EMCV infection. Although a lot of $CD11b^+TLR4^+$ cells were contained in MNCs from the heart at 5 days after EMCV infection, few $CD11c^+$, $CD3^+$, $CD19^+$ and $CD49b^+$ cells were contained (Fig. 4B).

**LPS-induced TNF-α production in $CD11b^+$ cells from the heart *in vivo* and *in vitro*.** Because MNCs from the heart at 5 days after EMCV infection were mainly occupied by $CD11b^+$ cells, we evaluated the ability of LPS-induced TNF-α production in $CD11b^+$ cells *in vivo*. The mice were intravenously inoculated with brefeldin A (250 μg/mouse) and LPS (10 μg/mouse) at 5 days after EMCV infection, and MNCs from the heart were harvested at 1 h after LPS treatment. TNF-α producing cell in gated $CD11b^+$ cells on the basis of isotype control were increased by LPS treatment (Fig. 5A).

Table 1 | Effect of LPS on lethality in EMCV-infected mice

| Mouse | Days[a] | LPS (μg) | Lethality (dead/total) |
|---|---|---|---|
| Wild-type | 0 | 10 | 0/10 |
| Wild-type | 2 | 10 | 0/10 |
| Wild-type | 5 | 10 | 10/10 |

[a]Days after EMCV infection.

Table 2 | Effect of various dose of LPS on lethality

| Mouse | Days[a] | LPS (μg) | Lethality (dead/total) |
|---|---|---|---|
| Wild-type | 5 | 0 | 0/8 |
| Wild-type | 5 | 1 | 1/8 |
| Wild-type | 5 | 5 | 6/8 |
| Wild-type | 5 | 10 | 8/8 |

[a]Days after EMCV infection.

Table 3 | Effect of LPS on lethality in TNF-α KO mice and wild-type mice treated with anti-TNF-α antibody

| Mouse | Days[a] | LPS (μg) | Lethality (dead/total) |
|---|---|---|---|
| Wild-type | 0 | 10 | 0/8 |
| Wild-type | 5 | 10 | 8/8 |
| TNF-α KO | 0 | 10 | 0/8 |
| TNF-α KO | 5 | 10 | 0/8 |
| Wild-type + anti-TNF-α Ab | 5 | 10 | 0/5 |

[a]Days after EMCV infection.

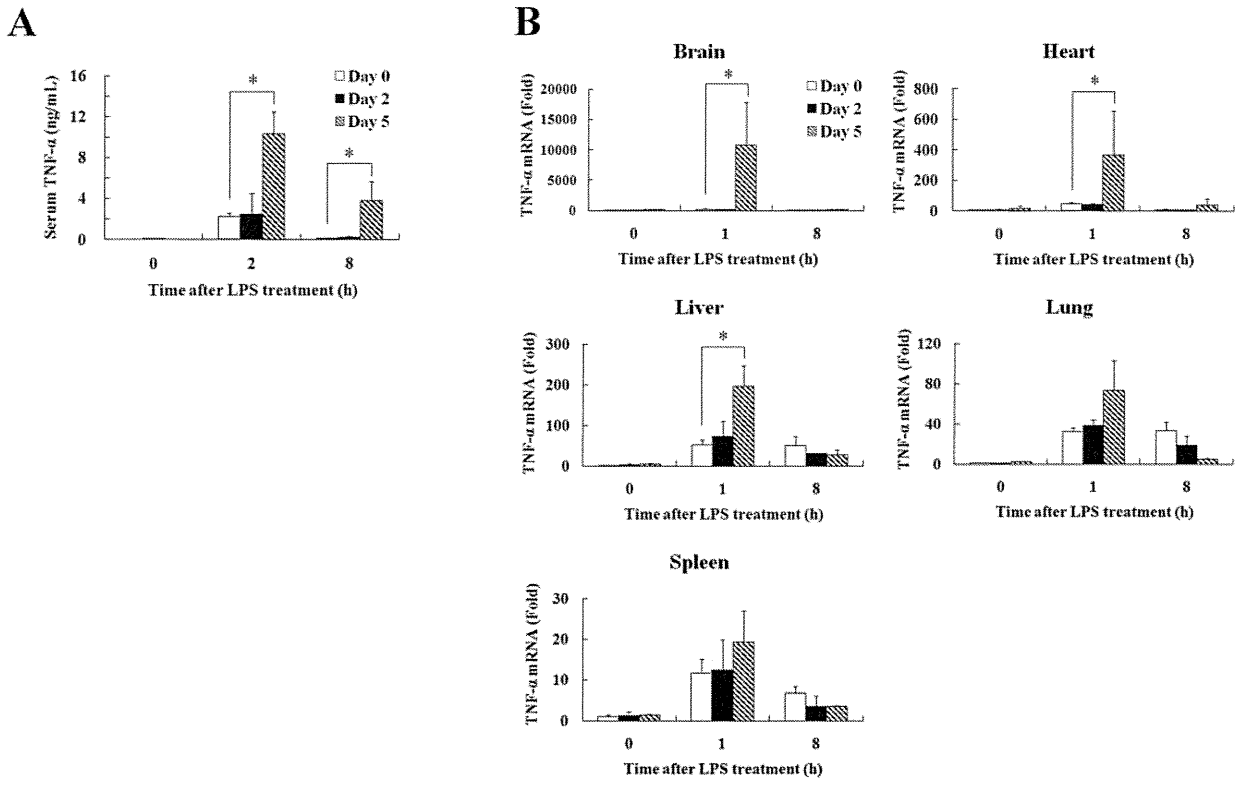


**Figure 1 | Effect of EMCV infection on LPS-induced TNF-α production.** The concentration of serum TNF-α was determined at 0, 2, and 8 h after LPS treatment in each EMCV infection period (A). TNF-α mRNA expression in the brain, heart, liver, lung, and spleen at 0, 1, and 8 h after LPS treatment in each EMCV infection period was determined on the basis of 18S rRNA expression using real-time RT-PCR. The data were calculated referring to mRNA levels of the respective tissues in control mice (0 days after EMCV infection, 0 hours after LPS inoculation) (B). The data are represented as means ± SD of the results of 4 mice in each group. *$p<0.05$

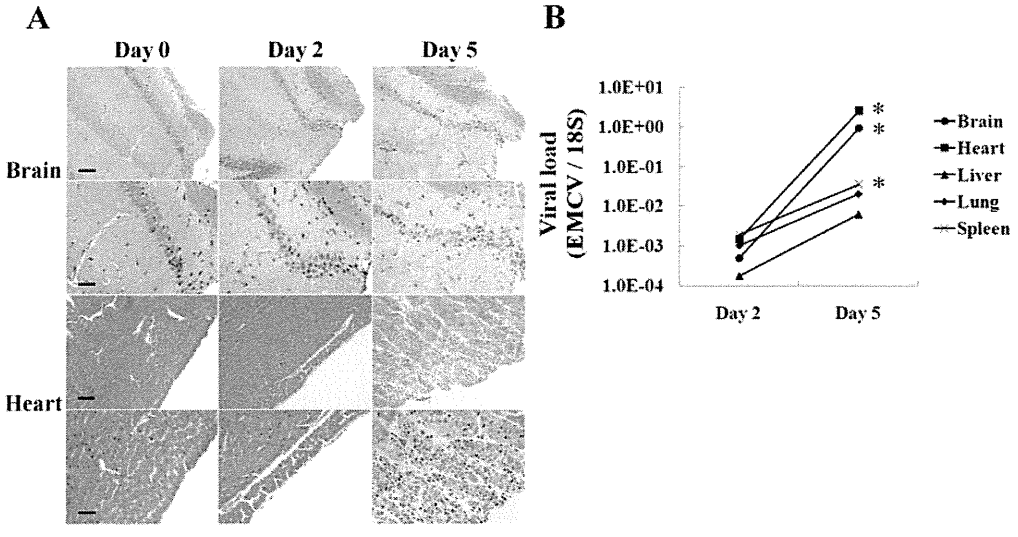


**Figure 2 | Histopathological finding and viral load of the tissues after EMCV infection.** Histopathological examination in the brain and heart at 0, 2 and 5 days after EMCV infection was performed. Tissue sections were deparaffinized, stained with hematoxylin-eosin, and examined under light microscopy. Scale bars, 200 μm (low-power field) and 50 μm (high-power field). These experiments were performed with 4 mice in each group and produced the same results (A). Viral RNA in the brain, heart, liver, lung, and spleen at 0, 2, and 5 days after EMCV infection was analyzed by real-time RT-PCR and was determined on the basis of 18S rRNA expression. The data are represented as means ± SD of the results of 4 mice in each group. The statistical analysis was performed by comparing with Day 2 (B). *$p<0.05$

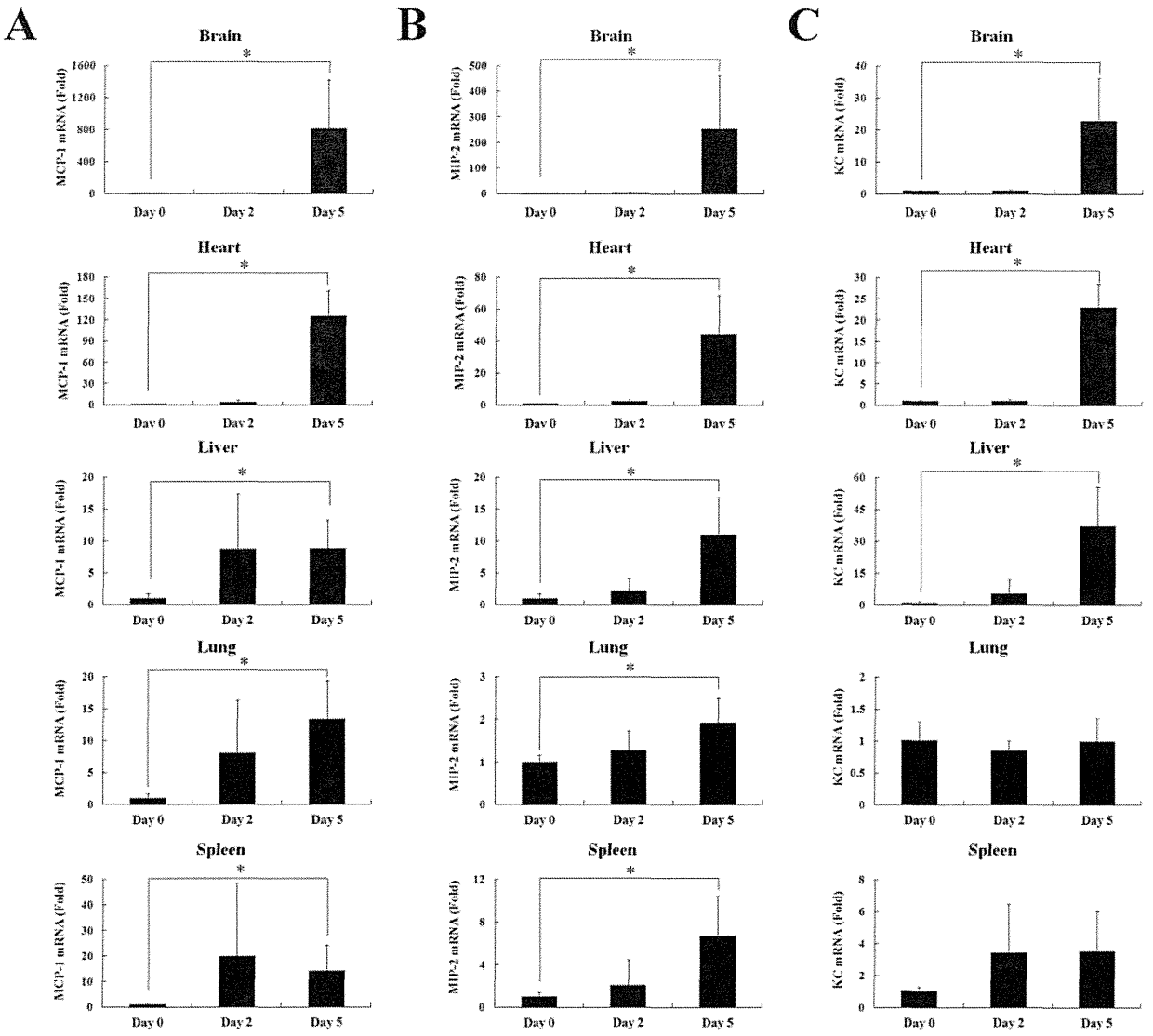


**Figure 3 | Effect of EMCV infection on mRNA expression of chemokines in the tissues.** The expression of MCP-1 (A), MIP-2 (B) and KC (C) mRNA in the brain, heart, liver, lung and spleen at 0, 2 and 5 days after EMCV infection was analyzed by real-time RT-PCR and was determined on the basis of 18S rRNA expression. The data were calculated referring to mRNA levels of the respective tissues in control mice (Day 0). The data are represented as means ± SD of the results of 6 mice in each group. *$p<0.05$

$CD11b^+$ and $CD11b^-$ cells from the heart at 5 days after EMCV infection were isolated by magnetic cell sorting. Isolated cells and total cells before isolation were cultured at $1\times10^5$ cells/200 μL with LPS (1 μg/mL) for 24 h. LPS-induced TNF-α production in $CD11b^+$ cells was significantly increased as compared with that in total cells and $CD11b^-$ cells. $CD11b^-$ cells could not produce TNF-α after LPS stimulation (Fig. 5B).

## Discussion

In this study, we demonstrated that LPS treatment at 5 days after EMCV infection induces an excess of TNF-α production in the brain and heart and lethal shock (Table 1, Fig. 1). Because this lethal effect of LPS was cancelled out in TNF-α KO mice infected with EMCV (Table 3), it is likely that TNF-α from the brain and heart plays a critical role in the lethal effect of LPS on EMCV infection. Septic shock is characterized by hypotension, decreased systemic vascular resistance and impaired vascular reactivity, and TNF-α has been implicated as a principal mediator in the pathogenesis of septic shock[23]. TNF-α is mainly produced by macrophages in the peripheral tissue after pathogen infection, and is involved in the elimination of pathogens from the host[24,25]. A protective role of TNF-α in EMCV-infected mouse model is previously reported[11]. In contrast, an excessive production of TNF-α induces hypothermia, hypotension, multiple organ failure, septic shock, and death[5,6]. In particular, previous reports demonstrated that the macrophages treated with some pre-stimulants produce a large amount of TNF-α on subsequent LPS stimulation. *Propionibacterium acnes*, an anaerobic gram-positive bacterium, exerts strong immunomodulatory activities, and participates in the formation of intrahepatic granulomas and induction of hypersensitivity for LPS in mice. Additionally, these activities depended on the recognition of bacteria via TLR9 and subsequent IL-12-mediated IFN-γ production[26,27]. EMCV infection also

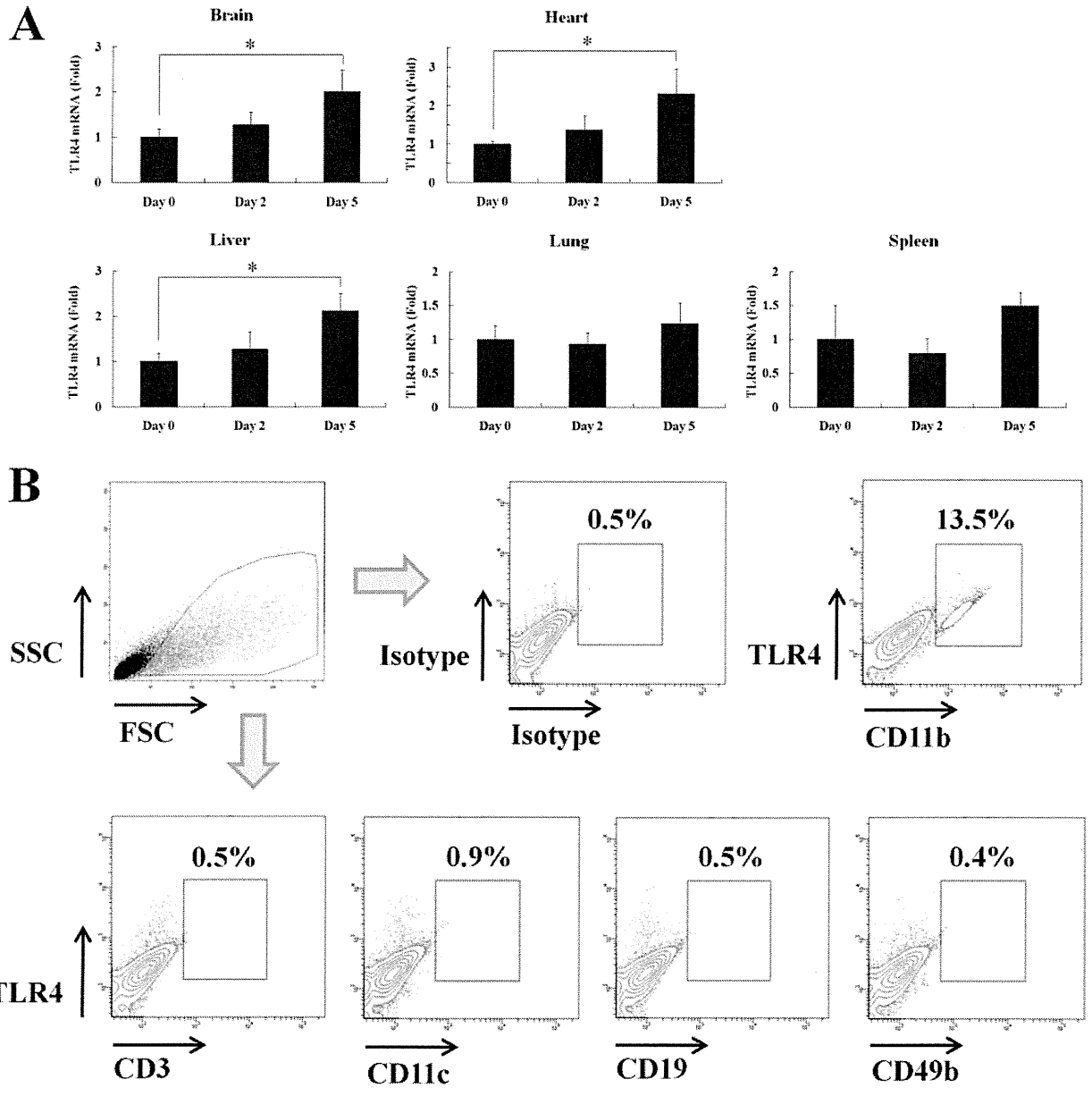


**Figure 4 | Effect of EMCV infection on TLR4 mRNA expression in tissues and infiltrating cells in the heart.** The expression TLR4 mRNA in the brain, heart, liver, lung, and spleen at 0, 2, and 5 days after EMCV infection was analyzed by real-time RT-PCR and was determined on the basis of 18S rRNA expression. The data were calculated referring to mRNA levels of the respective tissues in control mice (Day 0). The data are represented means ± SD from 4 mice of each group (A). Following reaction with anti-CD16/CD32 antibody to suppress nonspecific binding, MNCs from the heart were stained with anti-CD3ε, anti-CD11b, anti-CD11c, anti-CD19, anti-CD49b and anti-TLR4 antibody. The positive rate of the cells was made on the basis of isotype control. The data are representative of three separate experiments (B). *$p<0.05$

markedly increased the LPS-induced TNF-α mRNA level and viral road in the brain and heart (Fig. 1B, 2B). Namely, the susceptibility to LPS was enhanced in the EMCV-infected site.

TLR4 recognizes LPS from gram-negative bacteria, and its recognition is essential for the activation of the innate immune system. In humans with myocarditis, TLR4 mRNA is also increased in the heart[28]. In the present study, the mRNA expression of TLR4 in the brain, heart, and liver was increased after EMCV infection (Fig. 4A), and a significant increase in TNF-α mRNA expression was also confirmed after subsequent LPS stimulation (Fig. 1B). Histological findings revealed neuronal cell death and the presence of some inflammatory cells in hippocampus or brain surface of the brain, remarkable infiltration of inflammatory cells in the heart, and a little infiltration of inflammatory cells in the liver at 5 days after EMCV infection; further, the infiltrating cells were mainly composed of macrophages and neutrophils. These results indicate that the accumulation of inflammatory cells in the heart after EMCV infection is associated with this lethal septic shock model. In fact, there is a correlation between TLR4 mRNA expression and the number of infiltrated TLR4 positive cells in the heart. A previous report also

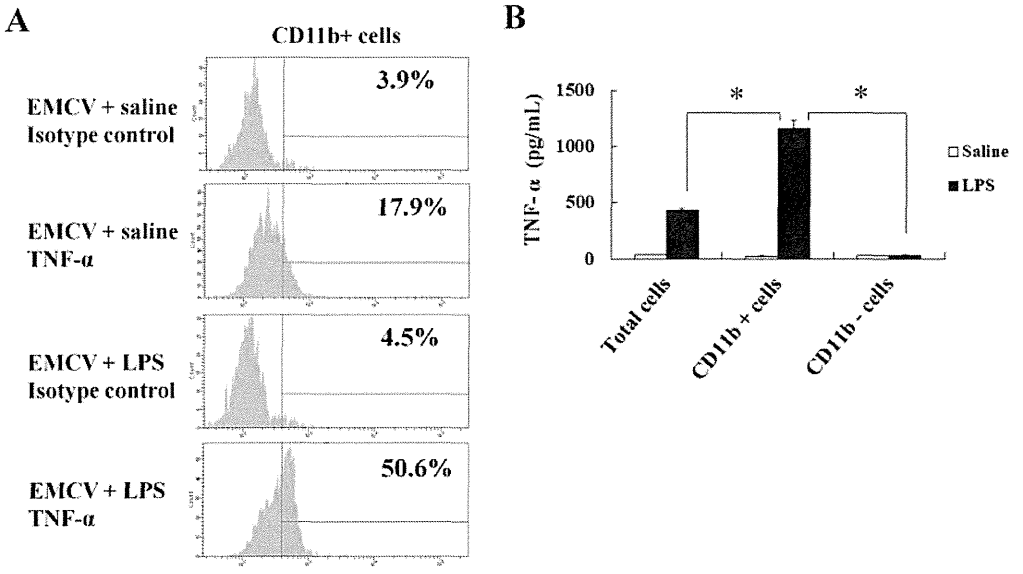


**Figure 5 | LPS-induced TNF-α production in CD11b$^+$ cells from the heart *in vivo* and *in vitro*.** The mice were inoculated intravenously with brefeldin A (250 μg/mouse) and LPS (10 μg/mouse) at 5 days after EMCV infection, and MNCs from the heart were harvested at 1 h after LPS treatment. MNCs were stained with anti-CD11b and anti-TNF-α antibody. The data are representative of three separate experiments (A). Isolated CD11b$^+$ and CD11b$^-$ MNCs and total cells before isolation were cultured at $1\times10^5$ cells per 200 μL with LPS (1 μg/mL) for 24 h. The concentration of TNF-α was determined in culture supernatant. The data are represented means ± SD in triplicate cultures (B). *$p<0.05$

demonstrated the augmentation of TLR4 mRNA expression by infiltration of TLR4-positive leukocytes into the liver in an IL-17-induced multiple tissue inflammation model[29]. Furthermore, our previous studies proved the infiltration of TLR4-positive leukocytes into the liver on α-galactosylceramide administration and the excessive response to subsequent LPS stimulation[8,15]. In this study, CD11b$^+$/TLR4$^+$ cells in the heart increased at 5 days after EMCV infection, but few CD11c$^+$, CD3$^+$, CD19$^+$ and CD49b$^+$ cells were contained (Fig. 4B). LPS-induced TNF-α was mainly produced by CD11b$^+$ cells in the heart at 5 days after EMCV infection *in vivo* and *in vitro* (Fig. 5). Therefore, it is suggested that the infiltration of CD11b$^+$ cells into the heart involves in the up-reguration of TLR4 mRNA and subsequent LPS induced TNF-α production.

mRNA expression of MCP-1, MIP-2, and KC in the brain and heart at 5 days after EMCV infection was markedly increased than that in uninfected mice (Fig. 3). The enhancement of the mRNA expression of these chemokines, especially MCP-1, may be involved in the infiltration of inflammatory cells into the heart. MCP-1 acts as a potent chemoattractant and activator of monocytes/macrophages[19,20]. Shiratsuchi et al[30] showed that macrophages phagocytose influenza virus-infected HeLa cells in a manner mediated by phosphatidylserine that appears on the surfaces of infected cells during the process of apoptosis. In addition, the inhibition of macrophage recruitment by MCP-1 augmented alveolar epithelial damage and apoptosis during influenza pneumonitis[31]. Thus, MCP-1 has an effective role in viral clearance, but it also may aggravate lethal shock by subsequent LPS stimulation under the EMCV-infected state.

Although the mice treated with 500 μg LPS died within 48 to 72 h in the general LPS-induced shock model[32,33], all mice treated with 10 μg LPS died within 24 hours in our model; this suggests that LPS susceptibility in mice markedly rises under the EMCV-infected condition. It is known that infection by the influenza virus, coxsackie virus, and adenovirus are involved in the onset of viral encephalitis or myocarditis[34,35], but there are few reports showing the effect of the secondary bacterial superimposed infection on viral encephalomyocarditis and its mechanism. In the present study, even a low-dose of LPS could cause the lethal septic shock in EMCV-infected mice. Thus, it is necessary to monitor serum endotoxin levels and prevent bacterial infection in patients with encephalitis and myocarditis.

In conclusion, we established a septic shock model using mice with viral encephalomyocarditis and demonstrated that the infiltration of CD11b$^+$ cells into tissues is involved in this lethal shock. From an immunological point of view, our animal model is useful for investigating the pathological state of bacterial superimposed infection on viral encephalomyocarditis.

## Methods

**Reagents.** LPS from *Escherichia coli* O111:B5 and brefeldin A were purchased from Sigma-Aldrich (St Louis, MO, USA). Mouse TNF-α antibody (monoclonal rat IgG1) for neutralize was purchased from R&D Systems (Minneapolis, MN, USA).

**Mice.** Mouse experiments were performed according to the guidelines of the Animal Ethics Committee of Gifu University Graduate School of Medicine. C57BL/6J mice aged approximately 8–10 weeks were obtained from Japan SLC (Hamamatsu, Japan) and used as wild-type (WT) mice. TNF-α gene knockout (TNF-α KO) mice of a C57BL/6J background were produced by gene targeting as described previously[11,36,37].

**Viral inoculation and LPS treatment.** A myocarditic variant of EMCV was generously provided by Dr. Seto (Keio University, Tokyo, Japan). The virus stock was stored at −80°C in Hanks' balanced salt solution (HBSS) with 0.1% BSA required for use. The mice were inoculated intraperitoneally with 20 pfu of EMCV in 0.2 mL saline and were treated intravenously with 10 μg LPS in 0.2 mL saline at 0 (non-infected), 2, and 5 days after the viral inoculation unless otherwise noted. The lethality was determined at 24 h after LPS treatment. The experiments were performed according to the institutional guidelines of Gifu University for microbiologic study.

**Measurement of serum TNF-α concentration.** The concentration of TNF-α in the serum and culture supernatant was determined using a mouse TNF-α Quantikine ELISA kit (R&D Systems, Minneapolis, MN, USA), according to the manufacturer's recommendations.

**Real-time RT-PCR analysis.** Real-time RT-PCR was used to quantify the levels of TNF-α, TLR4, MCP-1, MIP-2, KC mRNA, and EMCV RNA. Total RNA in the brain, heart, liver, lung and spleen was isolated using Isogen (Nippon Gene, Tokyo, Japan) and transcribed to cDNA by using the High capacity cDNA transcription kit (Applied Biosystems, Foster City, CA, USA). Purified cDNA was used as the template for real-time PCR conducted using pre-designed primer/probe sets for TNF-α, TLR4, MCP-1, MIP-2, KC and 18S rRNA (Applied Biosystems), according to the manufacturer's recommendations. The determination of EMCV RNA was performed by the use of the LightCycler DNA Master SYBR Green I (Roche Diagnostic Systems, Indianapolis,

IN, USA) and the following oligonucleotide primer pairs: EMCV sense, 5′-GTCGTGAAGGAAGCAGTTCC-3′, antisense, 5′-CACGTGGCTTTTGGCCGCAGAGGC-3′[11]. 18S rRNA was used as an internal control. Real-time PCR was carried out using a Light-Cycler rapid thermal cycler system (Roche Diagnostic Systems).

**Histological examination.** Histopathological examination of the brain and heart was performed at 0, 2, and 5 days after EMCV infection. The tissues were fixed in 10% formalin in PBS for 48 h and embedded in paraffin. Tissue sections were deparaffinized, stained with H&E, and examined under light microscopy.

**Cell isolation in heart.** Single cells from the heart, particularly non-parenchymal cells, were isolated in reference to a previous report[38]. The heart was minced with scissors and was shaken with 5 mL HBSS containing collagenase type 2 (600 U/mL) and deoxyribonuclease I (60 U/mL) (Worthington, Lakewood, NJ, USA) for 30 min at 37°C. The specimen was filtered through a stainless steel mesh, and red blood cells were lysed. After washing and filtration through a 70-μm cell strainer, the single cells were suspended in RPMI 1640 medium (Wako Pure Chemical Industries; Osaka, Japan) containing 10% heat-inactivated fetal bovine serum (Thermo Fisher Scientific Inc, Waltham, MA, USA) and cultured at 37°C in a 5% $CO_2$ atmosphere.

**Flow cytometry analysis.** MNCs from the heart at 5 days after EMCV infection were obtained by centrifugation of the single cells with Ficoll-Conray (IBL, Gunma, Japan). Flow cytometry was used to evaluate the expression level of CD3, CD11b, CD11c, CD19, CD49b and TLR4 in MNCs from the heart at 5 days after EMCV infection. Following reaction with anti-CD16/CD32 antibody to suppress nonspecific binding, MNCs were stained with FITC-conjugated hamster anti-mouse CD3ε antibody (clone 145-2C11; BD Biosciences, Franklin Lakes, NJ, USA), FITC-conjugated rat anti-mouse CD11b antibody (clone M1/70; eBioscience, San Diego, CA, USA), FITC-conjugated hamster anti-mouse CD11c antibody (clone HL-3; BD Biosciences), FITC-conjugated mouse anti-mouse CD19 antibody (clone MB19-1; eBioscience), FITC-conjugated rat anti-mouse CD49b antibody (clone DX5; eBioscience), and PE-conjugated rat anti-mouse TLR4/MD2 complex antibody (clone MTS510; eBioscience). The positive rate of the cells was made on the basis of isotype control. The phenotypic characterization of the cells was carried out using FACSCanto II (BD Biosciences).

**Intracellular cytokine staining *in vivo*.** The mice were intravenously inoculated with brefeldin A (250 μg/mouse) and LPS (10 μg/mouse) at 5 days after EMCV infection. MNCs from the heart at 1 h after LPS treatment were fixed and permeabilized with the Cytofix/Cytoperm buffer (BD Biosciences) and were stained with PE-conjugated rat anti-TNF-α antibody (clone MP6-XT22; eBioscience). The cells were analyzed using FACSCanto II (BD Biosciences).

**Isolation of $CD11b^+$ cells.** MNCs from the heart obtained at 5 days after EMCV infection were separated into $CD11b^+$ and $CD11b^-$ cells using anti-CD11b-conjugated magnetic beads (Miltenyi Biotec GmbH, Bergisch Gladbach, Germany). The magnetically labeled cells were purified using the QuadroMACS separation unit attached to a MACS multistand and LS columns (Miltenyi Biotec GmbH).

**Statistical analysis.** In each experiment, the results were expressed as the mean ± SD. The statistical significance of the difference in mean values was determined by Student's *t* test or one-way analysis of variance followed by Scheffe's test. *P* values of less than 0.05 were considered significant.


1. Bakaletz, L. O. Developing animal models for polymicrobial diseases. *Nat. Rev. Microbiol.* **2**, 552–568 (2004).
2. Brundage, J. F. Interactions between influenza and bacterial respiratory pathogens: implications for pandemic preparedness. *Lancet Infect. Dis.* **6**, 303–312 (2006).
3. Cohen, J. The immunopathogenesis of sepsis. *Nature* **420**, 885–891 (2002).
4. Bannerman, D. D. & Goldblum, S. E. Direct effects of endotoxin on the endothelium: barrier function and injury. *Lab Invest* **79**, 1181–1199 (1999).
5. Tracey, K. J. & Cerami, A. Tumor necrosis factor: a pleiotropic cytokine and therapeutic target. *Annu Rev Med* **45**, 491–503 (1994).
6. Brouckaert, P. & Fiers, W. Tumor necrosis factor and the systemic inflammatory response syndrome. *Curr Top Microbiol Immunol* **216**, 167–187 (1996).
7. Gumenscheimer, M., Mitov, I., Galanos, C. & Freudenberg, M. A. Beneficial or deleterious effects of a preexisting hypersensitivity to bacterial components on the course and outcome of infection. *Infect Immun* **70**, 5596–5603 (2002).
8. Ito, H. *et al.* Lethal endotoxic shock using alpha-galactosylceramide sensitization as a new experimental model of septic shock. *Lab Invest* **86**, 254–261 (2006).
9. Kishimoto, C., Kuribayashi, K., Masuda, T., Tomioka, N. & Kawai, C. Immunologic behavior of lymphocytes in experimental viral myocarditis: significance of T lymphocytes in the severity of myocarditis and silent myocarditis in BALB/c-nu/nu mice. *Circulation* **71**, 1247–1254 (1985).
10. Topham, D. J., Adesina, A., Shenoy, M., Craighead, J. E. & Sriram, S. Indirect role of T cells in development of polioencephalitis and encephalomyelitis induced by encephalomyocarditis virus. *J Virol* **65**, 3238–3245 (1991).
11. Wada, H. *et al.* Tumor necrosis factor-alpha (TNF-alpha) plays a protective role in acute viralmyocarditis in mice: A study using mice lacking TNF-alpha. *Circulation* **103**, 743–749 (2001).
12. Yamamoto, K. *et al.* Attenuation of virus-induced myocardial injury by inhibition of the angiotensin II type 1 receptor signal and decreased nuclear factor-kappa B activation in knockout mice. *J Am Coll Cardiol* **42**, 2000–2006 (2003).
13. Nasu-Nishimura, Y. *et al.* Cellular prion protein prevents brain damage after encephalomyocarditis virus infection in mice. *Arch Virol* **153**, 1007–1012 (2008).
14. Ito, H. *et al.* Augmentation of lipopolysaccharide-induced nitric oxide production by alpha-galactosylceramide in mouse peritoneal cells. *J Endotoxin Res* **11**,213–219 (2005).
15. Ohtaki, H. *et al.* Valpha14 NKT cells activated by alpha-galactosylceramide augment lipopolysaccharide-induced nitric oxide production in mouse intra-hepatic lymphocytes. *Biochem Biophys Res Commun* **378**, 579–583 (2009).
16. Ohtaki, H. *et al.* Interaction between LPS-induced NO production and IDO activity in mouse peritoneal cells in the presence of activated Valpha14 NKT cells. *Biochem Biophys Res Commun* **389**, 229–234 (2009).
17. Fejer, G. *et al.* Adenovirus infection dramatically augments lipopolysaccharide-induced TNF production and sensitizes to lethal shock. *J Immunol* **175**, 1498–1506 (2005).
18. Nansen, A. & Randrup Thomsen, A. Viral infection causes rapid sensitization to lipopolysaccharide: central role of IFN-alpha beta. *J Immunol* **166**, 982–988 (2001).
19. Matsushima, K., Larsen, C. G., DuBois, G. C. & Oppenheim, J. J. Purification and characterization of a novel monocyte chemotactic and activating factor produced by a human myelomonocytic cell line. *J Exp Med* **169**, 1485–1490 (1989).
20. Jiang, Y., Beller, D. I., Frendl, G. & Graves, D. T. Monocyte chemoattractant protein-1 regulates adhesion molecule expression and cytokine production in human monocytes. *J Immunol* **148**, 2423–2428 (1992).
21. Driscoll, K. E. Macrophage inflammatory proteins: biology and role in pulmonary inflammation. *Exp Lung Res* **20**, 473–490 (1994).
22. Lira, SA. *et al.* Expression of the chemokine N51/KC in the thymus and epidermis of transgenic mice results in marked infiltration of a single class of inflammatory cells. *J Exp Med* **180**, 2039–2048 (1994).
23. Tracey, K. J. *et al.* Anti-cachectin/TNF monoclonal antibodies prevent septic shock during lethal bacteraemia. *Nature* **330**, 662–664 (1987).
24. Sergerie, Y., Rivest, S. & Boivin, G. Tumor necrosis factor-alpha and interleukin-1 beta play a critical role in the resistance against lethal herpes simplex virus encephalitis. *J Infect Dis* **196**, 853–860 (2007).
25. Bekker, L. G. *et al.* Immunopathologic effects of tumor necrosis factor alpha in murine mycobacterial infection are dose dependent. *Infect Immun* **68**, 6954–6961 (2000).
26. Tchaptchet, S. *et al.* Innate, antigen-independent role for T cells in the activation of the immune system by Propionibacterium acnes. *Eur J Immunol* **40**, 2506–2516 (2010).
27. Inatsu, A. *et al.* Novel mechanism of C-reactive protein for enhancing mouse liver innate immunity. *Hepatology* **49**, 2044–2054 (2009).
28. Satoh, M. *et al.* Expression of Toll-like receptor 4 is associated with enteroviral replication in human myocarditis. *Clin Sci (Lond)* **104**, 577–584 (2003).
29. Tang, H. *et al.* TLR4 activation is required for IL-17-induced multiple tissue inflammation and wasting in mice. *J Immunol* **185**, 2563–2569 (2010).
30. Shiratsuchi, A., Kaido, M., Takizawa, T. & Nakanishi, Y. Phosphatidylserine-mediated phagocytosis of influenza A virus-infected cells by mouse peritoneal macrophages. *J Virol* **74**, 9240–9244 (2000).
31. Narasaraju, T., Ng, H. H., Phoon, M. C. & Chow, V. T. MCP-1 antibody treatment enhances damage and impedes repair of the alveolar epithelium in influenza pneumonitis. *Am J Respir Cell Mol Biol* **42**, 732–743 (2010).
32. Jung, ID. *et al.* Blockade of indoleamine 2,3-dioxygenase protects mice against lipopolysaccharide-induced endotoxin shock. *J Immunol* **182**, 3146–3154 (2009).
33. Liu, J. *et al.* The circadian clock Period 2 gene regulates gamma interferon production of NK cells in host response to lipopolysaccharide-induced endotoxic shock. *Infect Immun* **74**, 4750–4756 (2006).
34. Morishima, T. *et al.* Encephalitis and encephalopathy associated with an influenza epidemic in Japan. *Clin Infect Dis* **35**, 512–517 (2002).
35. Yajima, T. & Knowlton, KU. Viral myocarditis: from the perspective of the virus. *Circulation* **119**, 2615–2624 (2009).
36. Taniguchi, T., Takata, M., Ikeda, A., Momotani, E. & Sekikawa, K. Failure of germinal center formation and impairment of response to endotoxin in tumor necrosis factor alpha-deficient mice. *Lab Invest* **77**, 647–658 (1997).
37. Ito, H. *et al.* Role of TNF-alpha produced by nonantigen-specific cells in a fulminant hepatitis mouse model. *J Immunol* **182**, 391–397 (2009).
38. Pfister, O. *et al.* CD31- but Not CD31+ cardiac side population cells exhibit functional cardiomyogenic differentiation. *Circ Res* **97**, 52–61 (2005).


## Author contributions

HO, HI and MS designed the project. HO, HI, YO, AH, TI, HM, KS and MS designed experiments. HO, MH and MT performed the experimental work. HO, HI and MS prepared the manuscript and figures. All authors reviewed the manuscript.

## Additional information

**Competing financial interests:** The authors declare no competing financial interests.



**How to cite this article:** Ohtaki, H. *et al.* High susceptibility to lipopolysaccharide-induced lethal shock in encephalomyocarditis virus-infected mice. *Sci. Rep.* **2**, 367; DOI:10.1038/srep00367 (2012).

Journal of Medical Virology 84:438–444 (2012)

# Prevalence of Hepatitis C Virus Genotype 1a in Japan and Correlation of Mutations in the NS5A Region and Single-Nucleotide Polymorphism of Interleukin-28B With the Response to Combination Therapy With Pegylated-Interferon-Alpha 2b and Ribavirin

**Kazuhiko Hayashi,[1] Yoshiaki Katano,[1]* Teiji Kuzuya,[1] Yoshihiko Tachi,[1] Takashi Honda,[1] Masatoshi Ishigami,[1] Akihiro Itoh,[1] Yoshiki Hirooka,[1] Tetsuya Ishikawa,[1] Isao Nakano,[1] Fumihiro Urano,[2] Kentaro Yoshioka,[3] Hidenori Toyoda,[4] Takashi Kumada,[4] and Hidemi Goto[1]**

[1]*Department of Gastroenterology, Nagoya University Graduate School of Medicine, Showa-ku, Nagoya, Japan*
[2]*Department of Gastroenterology, Toyohashi Municipal Hospital, Toyohashi, Japan*
[3]*Division of Liver and Biliary Diseases, Department of Internal Medicine, Fujita Health University, Kutsukake-cho, Toyoake, Japan*
[4]*Department of Gastroenterology, Ogaki Municipal Hospital, Ogaki, Japan*

Hepatitis C virus (HCV) genotype 1a is rare in Japanese patients and the clinical characteristics of this genotype remain unclear. The interferon (IFN) sensitivity-determining region (ISDR) and single-nucleotide polymorphisms (SNPs) of interleukin-28B (IL28B) among patients with HCV genotype 1b are associated with IFN response, but associations among patients with genotype 1a are largely unknown. This study investigated the clinical characteristics of genotype 1a and examined whether genomic heterogeneity of the ISDR and SNPs of IL28B among patients with HCV genotype 1a affects response to combination therapy with pegylated-IFN-α2b and ribavirin. Subjects comprised 977 patients infected with HCV genotype 1, including 574 men and 412 women (mean age, 55.2 ± 10.6 years). HCV was genotyped by direct sequencing of the 5′-untranslated region and/or core regions and confirmed by direct sequencing of the NS5A region. HCV genotypes 1a (n = 32) and 1b (n = 945) were detected. Twenty-three (71.9%) of the 32 patients with genotype 1a were patients with hemophilia who had received imported clotting factors. Prevalence of genotype 1a after excluding patients with hemophilia was thus 0.9%. Of the 23 patients with genotype 1a who completed IFN therapy, 11 (47.8%) were defined as achieving sustained virological response. Factors related to sustained virological response by univariate analysis were IL28B and ISDR. In conclusion, HCV genotype 1a is rare in Japan. The presence of IL28B genotype TT, and more than two mutations, in the ISDR are associated with a good response to IFN therapy in patients with HCV genotype 1a. ***J. Med. Virol. 84:438–444, 2012.*** © 2012 Wiley Periodicals, Inc.

**KEY WORDS:** hepatitis C virus; genotype 1a; NS5A; IL 28B; interferon

## INTRODUCTION

Hepatitis C virus (HCV) is a member of the Flaviviridae family and causes chronic hepatitis that can develop into cirrhosis and hepatocellular carcinoma [Seeff, 2002]. HCV infection is a significant global health problem, affecting 170 million individuals worldwide. HCV can be divided into six genotypes and several subtypes according to genomic heterogeneity [Simmonds et al., 2005]. Each genotype shows a unique distribution and clinical characteristics such

All authors have nothing to disclose.

*Correspondence to: Yoshiaki Katano, MD, PhD, Department of Gastroenterology, Nagoya University Graduate School of Medicine, 65 Tsurumai-cho, Showa-ku, Nagoya 466-8550, Japan. E-mail: ykatano@med.nagoya-u.ac.jp

Accepted 23 November 2011
DOI 10.1002/jmv.23207
Published online in Wiley Online Library (wileyonlinelibrary.com).

as interferon (IFN) responsiveness [Ghany et al., 2009]. HCV genotypes 1b, 2a, and 2b are the major types encountered in Japan [Enomoto et al., 1990; Hayashi et al., 2003]. Genotype 1a is common worldwide, but is rare in Japan except among individuals with hemophilia who have received imported clotting factors [Fujimura et al., 1996; Otagiri et al., 2002; Hayashi et al., 2003]. The prevalence and clinical characteristics, including IFN responsiveness, of Japanese patients with HCV genotype 1a are unclear. HCV NS5A protein reportedly includes a domain associated with IFN response. This domain, located in the NS5A region of HCV genotype 1b, is closely associated with response to IFN therapy and is known as the IFN sensitivity-determining region (ISDR) [Enomoto et al., 1996]. IFN acts to inhibit viral replication by inducing double-stranded RNA-dependent protein kinase (PKR). The ISDR is located at the 5′ end of the PKR-binding domain and is inhibited by PKR in vitro [Gale et al., 1998]. ISDR heterogeneity of genotype 1b is thus an important factor that may affect response to IFN [Enomoto et al., 1996; Nakano et al., 1999; Pascu et al., 2004; Hayashi et al., 2011a]. Several studies have reported a relationship between ISDR and IFN responsiveness among patients with HCV genotype 1a [Hofgärtner et al., 1997; Zeuzem et al., 1997; Kumthip et al., 2011; Yahoo et al., 2011]. However, this remains controversial for genotype 1a, and the utility of ISDR sequences for predicting IFN responsiveness has not been investigated for HCV genotype 1a in Japan due to the rarity of this genotype. Both genetic heterogeneity of the HCV genome and host genetics contribute to IFN responsiveness. Several genome-wide association studies have thus been performed to clarify host factors associated with IFN responsiveness, revealing that interleukin-28B (IL28B) polymorphisms are strongly associated with response to IFN therapy [Ge et al., 2009; Suppiah et al., 2009; Tanaka et al., 2009; Thomas et al., 2009]. Combined use of the single-nucleotide polymorphisms (SNPs) of IL28B and amino acid substitutions in the core region and ISDR could thus improve the prediction of response to IFN in patients with HCV genotype 1b [Akuta et al., 2011; Hayashi et al., 2011b; Kurosaki et al., 2011]. However, the effects of a combined evaluation of the SNPs of IL28B and amino acid substitutions in the ISDR in patients with HCV genotype 1a on IFN response are unclear. The aim of the present study was to determine whether genomic heterogeneity of the ISDR and SNPs of IL28B among patients with HCV genotype 1a affect response to combination therapy with pegylated-IFN-α2b and ribavirin.

## PATIENTS AND METHODS

A total of 977 patients (569 men, 408 women) with chronic hepatitis C genotype 1 and high viral load (<100 KIU/ml) who were treated at Nagoya University Hospital and affiliated hospitals were enrolled in this study. Mean age of patients was 55.1 ± 12.2 years (range: 18–75 years). None of the patients had a history of chronic alcohol abuse, autoimmune disease, or metabolic disease. Patients with active intravenous drug use and immigrants were excluded from this study. The core region (aa 30–110) and ISDR (aa 2,209–2,248) of HCV were examined by direct sequencing. SNPs of IL28B (rs8099917) were identified using a real-time polymerase chain reaction (PCR) system. Patients received subcutaneous injections of pegylated-IFN-α2b (1.5 μg/kg) once each week along with oral ribavirin (600 mg/day for patients <60 kg, 800 mg/day for 60–80 kg, 1,000 mg/day for >80 kg) for 48 weeks. Patients who became negative for HCV-RNA between 16 and 36 weeks after initiating IFN treatment had the IFN treatment extended to 72 weeks, in accordance with Japanese guidelines [Kumada et al., 2010]. HCV-RNA levels in serum samples were examined at 12 weeks, at the end of IFN therapy, and at 6 months after the end of treatment. Serum was stored at −80°C for virological examination at pretreatment. Early virological response was defined as HCV-negative status at 12 weeks. Patients who were persistently negative for serum HCV-RNA at 24 weeks after withdrawal of IFN treatment were considered to show sustained virological response. Written informed consent was obtained from each patient, and the study protocol conformed to the ethical guidelines of the 1975 Declaration of Helsinki.

### Virological Analysis

HCV-RNA quantitative viremia load was determined by PCR. HCV was genotyped by direct sequencing of the 5′-untranslated region and/or core regions as described previously and confirmed by direct sequencing of the NS5A region [Otagiri et al., 2002; Dal Pero et al., 2007; Hayashi et al., 2011a]. Genotypes were classified according to the nomenclature proposed by Simmonds et al. [2005]. Direct sequencing of the core and NS5A-ISDR regions was performed as reported previously [Dal Pero et al., 2007; Hayashi et al., 2011a]. In brief, RNA was extracted from 140 μl of serum using a commercial kit (QIAamp Viral RNA Kit; Qiagen, Valencia, CA) and dissolved in 50 μl of diethylpyrocarbonate-treated water. RNA (10 ng) was used for reverse transcription with oligos and random hexamer primers with a commercial kit (iScript cDNA Synthesis Kit; Bio-Rad, Hercules, CA). The HCV core region and NS5A-ISDR were amplified by nested PCR. In brief, each 50-μl PCR reaction mixture contained 100 nM of each primer, 1 ng of template cDNA, 5 μl of GeneAmp 10× PCR buffer, 2 μl of dNTPs, and 1.25 U of AmpliTaq Gold (Applied Biosystems, Foster City, CA). Primers for the core region were: sense, 5′-GGGAGGTCTCGTAGACCGTGCACCATG-3′ and antisense, 5′-GAGMGGKATRTACCCCATGAGRTCGGC-3′. Primers for the NS5A-ISDR were: sense, 5′-GCCTGGAGCCCTTGTAGTC-3′ and

TABLE I. Clinical Characteristic of Patients With HCV Genotype 1a

| | N = 32 |
|---|---|
| Age (y.o.) | 36.4 ± 2.2 |
| Sex: male/female | 28/4 |
| AST (IU/L) | 48.8 ± 33.6 |
| ALT (IU/L) | 64.6 ± 57.8 |
| Platelet ($10^4/\mu l$) | 18.8 ± 6.0 |
| HCV RNA level (KIU/ml) | 2607.4 ± 3072.2 |
| Source (clotting factor/BTF/unknown) | 23/2/7 |

AST, aspartate aminotransferase; ALT, alanine aminotransferase; HCV, hepatitis C virus.

antisense, 5′-CTGCGTGAAGTGGTGGAATAC-3′. Amplification conditions consisted of 10 min at 94°C, followed by 40 cycles of 94°C for 10 sec, 55°C for 30 sec, and 72°C for 30 sec in a thermal cycler (GeneAmp PCR System 9700; Applied Biosystems). The second PCR was performed using the same reaction buffer with the first-round PCR product as template, and the following sets of primers: for the core region, sense primer 5′-AGACCGTGCACCATGAGCAC-3′ and antisense 5′-TACGCCGGGGGTCAKTRGGGCCCCA-3′; and for the NS5A-ISDR, sense 5′-TGTTTCCCCCACGCACTAC-3′ and antisense 5′-TGATGGGCAGTTTTTGTTCTTC-3′. PCR products were separated by electrophoresis on 2% agarose gels, stained with ethidium bromide, and visualized under ultraviolet light. PCR products were then purified and sequenced with the second-round PCR primers using a dye terminator sequencing kit (BigDye Terminator v1.1 Cycle Sequencing Kit; Applied Biosystems) and an ABI 310 DNA Sequencer (Applied Biosystems).

### Genotyping Analysis

Detection of SNPs for IL28B (rs8099917) was conducted using a real-time PCR system. In brief, genomic DNA was extracted from 150 μl of whole blood with a commercial kit (QIAamp DNA Blood mini Kit; Qiagen) and dissolved in 50 μl of diethylpyrocarbonate-treated water. DNA (10 ng) was used for PCR and genotyping of IL28B SNP (rs8099917) was performed by TaqMan allelic discrimination (ABI-Prism 7300 SDS software; Applied Biosystems) with TaqMan SNP Genotyping Assays provided by Applied Biosystems (C__11710096_10).

### Statistical Analysis

Data are expressed as mean ± standard deviation (SD). The paired *t*-test was used to analyze differences in variables. A value of $P < 0.05$ was considered statistically significant. Statview 5.0 software (SAS Institute, Cary, NC) was used for all analyses.

## RESULTS

Thirty-two of the 977 patients (3.3%) were infected by genotype 1a. Clinical characteristics of patients with genotype 1a are summarized in Table I. Twenty-three cases involved patients with hemophilia who had received imported clotting factors. The prevalence of genotype 1a after excluding patients with hemophilia was 0.9%. A comparison of clinical characteristics according to hemophilia status is shown in Table II. No significant differences were apparent among the two groups. Differences in clinical characteristics between genotypes 1a and 1b are shown in Table III. Males were more frequent among patients with genotype 1a (87.5%) than among those with genotype 1b (57.2%), as the majority of patients with genotype 1a were young male patients with hemophilia. Sequence alignments of the core region at codons 71 and 90 showed arginine and cysteine, respectively, in all patients. The HCV core region of genotype 1a was thus well-conserved, with no significant mutations at codons 71 or 90. This is not similar to previous findings for genotype 1b [Akuta et al., 2005, 2011; Hayashi et al., 2011a,b; Kurosaki et al., 2011]. Alignment of the amino acid sequence for NS5A-ISDR is shown in Figure 1. The sequence of the HCV-1 strain was defined as the consensus sequence of genotype 1a, and the number of mutations to the chosen consensus sequence in ISDR was used to analyze the ISDR system. Sequences of the HCV-1 strain and HCV-1 strain with only one amino acid substitution were defined as wild-type, while ISDR sequences with more than two amino acid substitutions were defined as mutant-type. Twenty-seven strains were defined as wild-type and 5 strains were defined as mutant-type. IL28B genotypes could be obtained for 25 patients, and IL28B alleles were TT (n = 14) and TG (n = 11). Twenty-three patients received pegylated-IFN-α2b plus ribavirin therapy. Twenty patients were treated for 48 weeks, and 1 patient was treated for 72 weeks. Two patients were withdrawn at 24 weeks due to a

TABLE II. Clinical Characteristic According to Hemophilia

| | Patients with hemophilia (N = 23) | Patients without hemophilia (N = 9) | *P*-value |
|---|---|---|---|
| Age (y.o.) | 37.1 ± 9.2 | 37.1 ± 16.3 | 0.9966 |
| Sex: male/female | 22/1 | 6/3 | 0.0572 |
| AST (IU/L) | 51.2 ± 34.8 | 41.9 ± 30.9 | 0.5072 |
| ALT (IU/L) | 68.2 ± 55.8 | 54.0 ± 66.1 | 0.5566 |
| Platelet ($10^4/\mu l$) | 18.4 ± 6.8 | 19.8 ± 3.0 | 0.5602 |
| HCV levels (KIU/ml) | 2599.6 ± 3108.0 | 2630.0 ± 3176.5 | 0.9812 |

AST, aspartate aminotransferase; ALT, alanine aminotransferase; HCV, hepatitis C virus.

TABLE III. Clinical Characteristic According to Genotypes

| | Genotype 1a (N = 32) | Genotype 1b (N = 945) | *P*-value |
|---|---|---|---|
| Age (y.o.) | 36.4 ± 2.2 | 55.9 ± 11.6 | 0.0001 |
| Sex: male/female | 28/4 | 546/408 | 0.0004 |
| Patients with hemophilia | 23 | 4 | 0.0001 |
| AST (IU/L) | 48.8 ± 33.6 | 59.9 ± 45.0 | 0.1745 |
| ALT (IU/L) | 64.6 ± 57.8 | 64.6 ± 57.8 | 0.9894 |
| Platelet ($10^4/\mu l$) | 18.8 ± 6.0 | 17.2 ± 6.0 | 0.0918 |
| HCV levels (KIU/ml) | 2607.4 ± 3072.2 | 2011.5 ± 1453.8 | 0.0642 |

AST, aspartate aminotransferase; ALT, alanine aminotransferase; PLT, platelet count; HCV, hepatitis C virus.

lack of response to IFN therapy. Frequency of early virological response, characterized by undetectable HCV at 12 weeks, was 30.4% (7/23). Virological response rate at the end of treatment was 47.8% (11/23). Finally, 11 of 23 patients (47.8%) achieved sustained virological response. Clinical characteristics were compared between patients who achieved sustained virological response and patients who did not (Table IV), revealing significant differences in two factors on univariate analysis: IL28B and ISDR.

## DISCUSSION

The present study investigated 977 patients with genotype 1 using direct sequencing of core and NS5A regions, revealing that genotype 1a is rare (3.3%) in Japan. Of the 33 patients with genotype 1a, 23 (71.9%) were patients with hemophilia, confirming that the majority of cases with genotype 1a involve patients with hemophilia who have received imported clotting factors, as previously reported [Fujimura et al., 1996; Otagiri et al., 2002; Hayashi et al., 2003]. Analysis after excluding patients with hemophilia revealed the prevalence of genotype 1a in Japan was 0.9% (9/954). Recently, the distributions of HBV genotypes have been changing in Japan due to international exchange [Hayashi et al., 2007; Matsuura et al., 2009]. However, prevalences of HCV genotypes have remained stable because of the different modes of infection involved. The present study revealed that 11 (47.8%) of 23 patients achieved sustained virological response. The IFN responsiveness of HCV genotype 1a in Japanese patients was reported in 1999 from Okinawa, a far southern island in Japan [Sakugawa et al., 1997]. That study reported that the rate of sustained virological response tended to be higher in patients with genotype 1a than in those with genotype 1b, but no significant differences were identified because of the small number of patients with genotype 1a. Low virological response rates in both genotypes 1a and 1b were confirmed in the present Japanese patients, as in Caucasian patients [Manns et al., 2001; McHutchison et al., 2009]. No significant differences in sustained virological response rate were seen between genotypes 1a and 1b. Discriminating between genotypes 1a and 1b thus seems to have little clinical relevance in terms of IFN responsiveness. Viral factors associated with sustained virological response, including HCV genotype, have been studied most frequently studied and mutations in the core and NS5A regions of HCV genotype 1b have been associated with response to IFN therapy [Akuta et al., 2005, 2010, 2011; Okanoue et al., 2009; Nakagawa et al., 2010; Toyoda et al., 2010; Hayashi et al., 2011a; Hayes et al., 2011; Kumthip et al., 2011; Kurosaki et al., 2011]. These viral factors could improve prediction of sustained virological response for genotype 1a, as in 1b. Amino acid substitutions at positions 70 and 91 of the HCV core region in genotype 1b have been related to IFN responsiveness, liver steatosis, hepatic oxidative stress, insulin resistance, and carcinogenesis [Akuta et al., 2005, 2007, 2009; Tachi et al., 2010]. These substitutions may have substantial impacts on

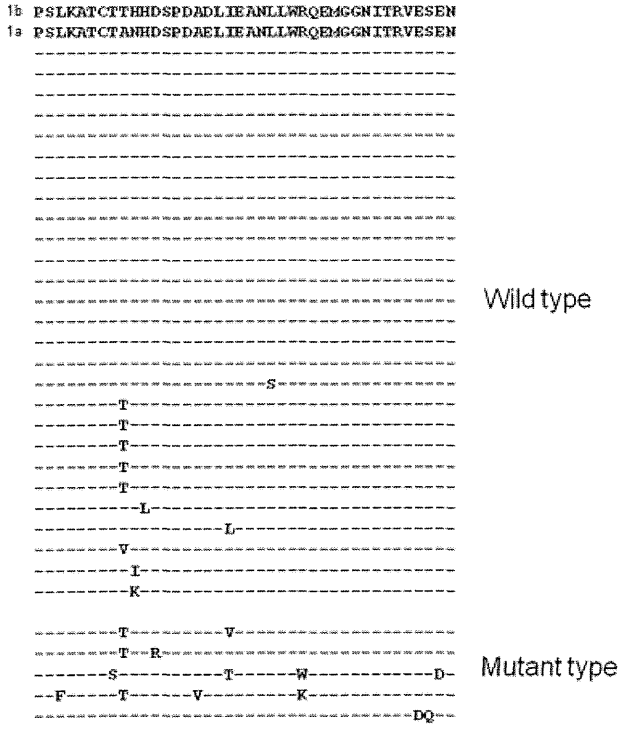


Fig. 1. Alignment of the amino acid sequence for the NS5A-ISDR. In the sequence alignment, dashes indicate amino acids identical to consensus sequence HCV1. Sequences of the HCV1 strain and HCV1 strains with one-nucleotide substitutions were defined as wild-type ISDR, and all other strains were defined as mutant-type ISDR. ISDR, interferon sensitivity-determining region.

TABLE IV. Univariate Analysis: Factors Predictive of Sustained Virologic Response

| Factors | Sustained virologic response (n = 11) | Non-sustained virologic response (n = 12) | *P*-value |
|---|---|---|---|
| Age (y.o.) | 37.9 ± 10.9 | 39.8 ± 11.3 | 0.6958 |
| Gender: male/female | 10/1 | 10/2 | 0.9999 |
| ALT (IU/L) | 78.2 ± 50.8 | 62.6 ± 68.1 | 0.5435 |
| AST (IU/L) | 51.4.4 ± 29.2 | 48.8 ± 40.4 | 0.8616 |
| PLT ($\times 10^4/mm^3$) | 19.0 ± 5.4 | 19.3 ± 5.7 | 0.8870 |
| HCV RNA level (KIU/ml) | 1323.1 ± 1077.3 | 2567.0 ± 2940.8 | 0.2481 |
| ISDR: wild/mutant | 7/4 | 12/0 | 0.0373 |
| IL28B:TT/TG | 9/1 | 4/8 | 0.0115 |

AST, aspartate aminotransferase; ALT, alanine aminotransferase; PLT, platelet count; HCV, hepatitis C virus; ISDR, interferon sensitivity-determining region; IL28B, interleukin 28B.

the pathogenesis of HCV genotype 1a infection. However, the HCV core region of genotype 1a is well-conserved and no significant mutations were seen in the core region, which is associated with IFN responsiveness. Several reports have also found that the HCV core region, including positions 70 and 91, of HCV genotype 1a is highly conserved [Alestig et al., 2011; Kumthip et al., 2011]. Mutations in the core region of genotype 1a would be rare, so this region might be unsuitable for routine clinical use, unlike in genotype 1b. However, the number of patients in this study was small, and large studies including from other countries are needed to clarify these issues. The ISDR in the NS5A region of HCV genotype 1b is closely associated with response to IFN therapy. ISDR mutations of genotype 1b are well known to be more important in predicting sustained virological response in Japanese patients than European patients [Hofgärtner et al., 1997; Zeuzem et al., 1997; Nakano et al., 1999; Pascu et al., 2004; Hayashi et al., 2011a]. European studies have failed to detect the specific amino acid substitutions in ISDR of genotype 1a associated with IFN responsiveness [Hofgärtner et al., 1997; Zeuzem et al., 1997]. In this study, sustained virological response was achieved in 36.8% of patients with wild-type ISDR and 100% of patients with mutant-type ($P = 0.0373$). The present analysis showed a close relationship between ISDR of genotype 1a and sustained virological response, as in genotype 1b. Recent investigations in Thailand and Iran have failed to identify the usefulness of ISDR for HCV genotype 1a in predicting sustained virological response [Kumthip et al., 2011; Yahoo et al., 2011]. The high virological response rate and low prevalence of patients with mutations in the ISDR do not favor the use of ISDR analysis in predicting IFN responsiveness [Herion and Hoofnagle, 1997; Yokozaki et al., 2011]. Rates of sustained virological response among these studies were much higher than those in the present study (68.4% and 75% vs. 47.8%). The mean number of mutations in patients who achieved sustained virological response in the studies by Kumthip et al. [2011] and Yahoo et al. [2011], and the present group were 1.4, 1.4, and 1.6, respectively. Differences in sustained virological response and the number of mutations to the ISDR might underpin this discrepancy in the evaluation of ISDR. Although the sample size in the present study was small, the results indicate that ISDR represents a strong indicator of progression to sustained virological response for patients with HCV genotype 1a. Amino acid substitutions in the ISDR of genotype 1a thus also play an important role in predicting sustained virological response in Japanese patients compared to patients from other countries. IL28B polymorphisms such as host genetics, as well as mutations in the HCV genome, contribute to IFN treatment outcomes. Rates of sustained virological response in patients in this study with TT and TG were 69.2% and 11.1%, respectively. The TG allele of the IL28B genotype was significantly associated with poor response to IFN therapy ($P = 0.0115$). SNPs of IL28B would regulate the expression of IFN-stimulated genes and affect IFN responsiveness. IL28B and ISDR thus exert independent effects on IFN responsiveness and both host and viral factors impacting IFN responsiveness would improve the prediction of sustained virological response. Several studies have thus reported that both the SNP of IL28B and mutations in the ISDR were associated with sustained virological response in patients with HCV genotype 1b [Akuta et al., 2011; Hayashi et al., 2011b; Kurosaki et al., 2011]. In the present study of HCV genotype 1a, among the 9 patients who had simultaneously the TG allele for IL28B and wild-type ISDR, only 1 achieved sustained virological response (11.1%). The best-sustained virological response was achieved in patients with mutant-type ISDR and the T allele (100%). The combination of SNPs for IL28B and mutations in ISDR may thus predict response to IFN therapy in patients with HCV genotype 1a as well as genotype 1b. Given the small sample size in this investigation, larger cohorts are needed to confirm the present results. Furthermore, infection with genotype 1a in Japanese patients is rare, making large-scale studies difficult to perform.

In conclusion, the prevalence of HCV genotype 1a is rare in Japan and the majority of cases involve patients with hemophilia. The TG genotype of IL28B is associated with poor response, while mutant-type ISDR is associated with good response to combination therapy with pegylated-IFN-α2b and ribavirin in patients with HCV genotype 1a. Combined use of both IL28B and ISDR could improve the prediction of IFN response.

## REFERENCES


Akuta N, Suzuki F, Sezaki H, Suzuki Y, Hosaka T, Someya T, Kobayashi M, Saitoh S, Watahiki S, Sato J, Matsuda M, Kobayashi M, Arase Y, Ikeda K, Kumada H. 2005. Association of amino acid substitution pattern in core protein of hepatitis C virus genotype 1b high viral load and non-virological response to interferon-ribavirin combination therapy. Intervirology 48:372–380.

Akuta N, Suzuki F, Kawamura Y, Yatsuji H, Sezaki H, Suzuki Y, Hosaka T, Kobayashi M, Kobayashi M, Arase Y, Ikeda K, Kumada H. 2007. Amino acid substitutions in the hepatitis C virus core region are the important predictor of hepatocarcinogenesis. Hepatology 46:1357–1364.

Akuta N, Suzuki F, Hirakawa M, Kawamura Y, Yatsuji H, Sezaki H, Suzuki Y, Hosaka T, Kobayashi M, Kobayashi M, Saitoh S, Arase Y, Ikeda K, Kumada H. 2009. Amino acid substitutions in the hepatitis C virus core region of genotype 1b are the important predictor of severe insulin resistance in patients without cirrhosis and diabetes mellitus. J Med Virol 81:1032–1039.

Akuta N, Suzuki F, Hirakawa M, Kawamura Y, Yatsuji H, Sezaki H, Suzuki Y, Hosaka T, Kobayashi M, Kobayashi M, Saitoh S, Arase Y, Ikeda K, Chayama K, Nakamura Y, Kumada H. 2010. Amino acid substitution in hepatitis C virus core region and genetic variation near the interleukin 28B gene predict viral response to telaprevir with peginterferon and ribavirin. Hepatology 52:421–429.

Akuta N, Suzuki F, Hirakawa M, Kawamura Y, Sezaki H, Suzuki Y, Hosaka T, Kobayashi M, Kobayashi M, Saitoh S, Arase Y, Ikeda K, Chayama K, Nakamura Y, Kumada H. 2011. Amino acid substitution in HCV core/NS5A region and genetic variation near IL28B gene affect treatment efficacy to interferon plus ribavirin combination therapy. Intervirology (in press).

Alestig E, Arnholm B, Eilard A, Lagging M, Nilsson S, Norkrans G, Wahlberg T, Wejstål R, Westin J, Lindh M. 2011. Core mutations, IL28B polymorphisms and response to peginterferon/ribavirin treatment in Swedish patients with hepatitis C virus genotype 1 infection. BMC Infect Dis 12:124.

Dal Pero F, Tang KH, Gerotto M, Bortoletto G, Paulon E, Herrmann E, Zeuzem S, Alberti A, Naoumov NV. 2007. Impact of NS5A sequences of hepatitis C virus genotype 1a on early viral kinetics during treatment with peginterferon-alpha 2a plus ribavirin. J Infect Dis 196:998–1005.

Enomoto N, Takada A, Nakao T, Date T. 1990. There are two major types of hepatitis C virus in Japan. Biochem Biophys Res Commun 170:1021–1025.

Enomoto N, Sakuma I, Asahina Y, Kurosaki M, Murakami T, Yamamoto C, Ogura Y, Izumi N, Marumo F, Sato C. 1996. Mutations in the nonstructural protein 5A gene and response to interferon in patients with chronic hepatitis C virus 1b infection. N Engl J Med 334:77–81.

Fujimura Y, Ishimoto S, Shimoyama T, Narita N, Kuze Y, Yoshioka A, Fukui H, Tanaka T, Tsuda F, Okamoto H, Miyakawa Y, Mayumi M. 1996. Genotypes and multiple infections with hepatitis C virus in patients with haemophilia A in Japan. J Viral Hepat 3:79–84.

Gale M, Jr., Blakely CM, Kwieciszewski B, Tan SL, Dossett M, Tang NM, Korth MJ, Polyak SJ, Gretch DR, Katze MG. 1998. Control of PKR protein kinase by hepatitis C virus nonstructural 5A protein: Molecular mechanisms of kinase regulation. Mol Cell Biol 18:5208–5218.

Ge D, Fellay J, Thompson AJ, Simon JS, Shianna KV, Urban TJ, Heinzen EL, Qiu P, Bertelsen AH, Muir AJ, Sulkowski M, McHutchison JG, Goldstein DB. 2009. Genetic variation in IL28B predicts hepatitis C treatment-induced viral clearance. Nature 461:399–401.

Ghany MG, Strader DB, Thomas DL, Seeff LB, American Association for the Study of Liver Diseases. 2009. Diagnosis, management, and treatment of hepatitis C: An update. Hepatology 49: 1335–1374.

Hayashi K, Fukuda Y, Nakano I, Katano Y, Toyoda H, Yokozaki S, Hayakawa T, Morita K, Nishimura D, Kato K, Urano F, Takamatsu J. 2003. Prevalence and characterization of hepatitis C virus genotype 4 in Japanese hepatitis C carriers. Hepatol Res 25:409–414.

Hayashi K, Katano Y, Takeda Y, Honda T, Ishigami M, Itoh A, Hirooka Y, Nakano I, Yano M, Goto H, Yoshioka K, Toyoda H, Kumada T. 2007. Comparison of hepatitis B virus subgenotypes in patients with acute and chronic hepatitis B and absence of lamivudine-resistant strains in acute hepatitis B in Japan. J Med Virol 79:366–373.

Hayashi K, Katano Y, Ishigami M, Itoh A, Hirooka Y, Nakano I, Urano F, Yoshioka K, Toyoda H, Kumada T, Goto H. 2011a. Mutations in the core and NS5A region of hepatitis C virus genotype 1b and correlation with response to pegylated-interferon-alpha 2b and ribavirin combination therapy. J Viral Hepat 18:280–286.

Hayashi K, Katano Y, Honda T, Ishigami M, Itoh A, Hirooka Y, Ishikawa T, Nakano I, Yoshioka K, Toyoda H, Kumada T, Goto H. 2011b. Association of interleukin 28B and mutations in the core and NS5A region of hepatitis C virus with response to peg-interferon and ribavirin therapy. Liver Int 9:1359–1365.

Hayes CN, Kobayashi M, Akuta N, Suzuki F, Kumada H, Abe H, Miki D, Imamura M, Ochi H, Kamatani N, Nakamura Y, Chayama K. 2011. HCV substitutions and IL28B polymorphisms on outcome of peg-interferon plus ribavirin combination therapy. Gut 60:261–267.

Herion D, Hoofnagle JH. 1997. The interferon sensitivity determining region: All hepatitis C virus isolates are not the same. Hepatolgy 25:769–770.

Hofgärtner WT, Polyak SJ, Sullivan DG, Carithers RL, Jr., Gretch DR. 1997. Mutations in the NS5A gene of hepatitis C virus in North American patients infected with HCV genotype 1a or 1b. J Med Virol 53:118–126.

Kumada H, Okanoue T, Onji M, Moriwaki H, Izumi N, Tanaka E, Chayama K, Sakisaka S, Takehara T, Oketani M, Suzuki F, Toyota J, Nomura H, Yoshioka K, Seike M, Yotsuyanagi H, Ueno Y, The Study Group for the Standardization of Treatment of Viral Hepatitis Including Cirrhosis, Ministry of Health, Labour and Welfare of Japan. 2010. Guidelines for the treatment of chronic hepatitis and cirrhosis due to hepatitis C virus infection for the fiscal year 2008 in Japan. Hepatol Res 40: 8–13.

Kumthip K, Pantip C, Chusri P, Thongsawat S, O'Brien A, Nelson KE, Maneekarn N. 2011. Correlation between mutations in the core and NS5A genes of hepatitis C virus genotypes 1a, 1b, 3a, 3b, 6f and the response to pegylated interferon and ribavirin combination therapy. J Viral Hepat 18:e117–e125.

Kurosaki M, Tanaka Y, Nishida N, Sakamoto N, Enomoto N, Honda M, Sugiyama M, Matsuura K, Sugauchi F, Asahina Y, Nakagawa M, Watanabe M, Sakamoto M, Maekawa S, Sakai A, Kaneko S, Ito K, Masaki N, Tokunaga K, Izumi N, Mizokami M. 2011. Pretreatment prediction of response to pegylated-interferon plus ribavirin for chronic hepatitis C using genetic polymorphism in IL28B and viral factors. J Hepatol 54:439–448.

Manns MP, McHutchison JG, Gordon SC, Rustgi VK, Shiffman M, Reindollar R, Goodman ZD, Koury K, Ling M, Albrecht JK. 2001. Peginterferon alfa-2b plus ribavirin compared with interferon alfa-2b plus ribavirin for initial treatment of chronic hepatitis C: A randomised trial. Lancet 358:958–965.

Matsuura K, Tanaka Y, Hige S, Yamada G, Murawaki Y, Komatsu M, Kuramitsu T, Kawata S, Tanaka E, Izumi N, Okuse C, Kakumu S, Okanoue T, Hino K, Hiasa Y, Sata M, Maeshiro T, Sugauchi F, Nojiri S, Joh T, Miyakawa Y, Mizokami M. 2009. Distribution of hepatitis B virus genotypes among patients with chronic infection in Japan shifting toward an increase of genotype A. J Clin Microbiol 47:1476–1483.

McHutchison JG, Lawitz EJ, Shiffman ML, Muir AJ, Galler GW, McCone J, Nyberg LM, Lee WM, Ghalib RH, Schiff ER, Galati JS, Bacon BR, Davis MN, Mukhopadhyay P, Koury K, Noviello S, Pedicone LD, Brass CA, Albrecht JK, Sulkowski MS, IDEAL Study Team. 2009. Peginterferon alfa-2b or alfa-2a with ribavirin for treatment of hepatitis C infection. N Engl J Med 361:580–593.

Nakagawa M, Sakamoto N, Ueyama M, Mogushi K, Nagaie S, Itsui Y, Azuma S, Kakinuma S, Tanaka H, Enomoto N, Watanabe M. 2010. Mutations in the interferon sensitivity determining region and virological response to combination therapy with pegylated-interferon alpha 2b plus ribavirin in patients with chronic hepatitis C-1b infection. J Gastroenterol 45:656–665.

Nakano I, Fukuda Y, Katano Y, Nakano S, Kumada T, Hayakawa T. 1999. Why is the interferon sensitivity-determining region (ISDR) system useful in Japan? J Hepatol 30:1014–1022.

Okanoue T, Itoh Y, Hashimoto H, Yasui K, Minami M, Takehara T, Tanaka E, Onji M, Toyota J, Chayama K, Yoshioka K, Izumi N, Akuta N, Kumada H. 2009. Predictive values of amino acid sequences of the core and NS5A regions in antiviral therapy for

hepatitis C: A Japanese multi-center study. J Gastroenterol 44: 952–963.

Otagiri H, Fukuda Y, Nakano I, Katano Y, Toyoda H, Yokozaki S, Hayashi K, Hayakawa T, Fukuda Y, Kinoshita M, Takamatsu J. 2002. Evaluation of a new assay for hepatitis C virus genotyping and viral load determination in patients with chronic hepatitis C. J Virol Methods 103:137–143.

Pascu M, Martus P, Höhne M, Wiedenmann B, Hopf U, Schreier E, Berg T. 2004. Sustained virological response in hepatitis C virus type 1b infected patients is predicted by the number of mutations within the NS5A-ISDR: A meta-analysis focused on geographical differences. Gut 53:1345–1351.

Sakugawa H, Nakasone H, Kinjo F, Saito A, Keida Y, Kikuchi K, Oyadomari Y, Ishihara M, Nakasone K, Yogi S, Kinjo Y, Taira M. 1997. Clinical features of patients with chronic liver disease associated with hepatitis C virus genotype 1a/I in Okinawa, Japan. J Gastroenterol Hepatol 12:176–181.

Seeff LB. 2002. Natural history of chronic hepatitis C. Hepatology 36:S35–S46.

Simmonds P, Bukh J, Combet C, Deléage G, Enomoto N, Feinstone S, Halfon P, Inchauspé G, Kuiken C, Maertens G, Mizokami M, Murphy DG, Okamoto H, Pawlotsky JM, Penin F, Sablon E, Shin-I T, Stuyver LJ, Thiel HJ, Viazov S, Weiner AJ, Widell A. 2005. Consensus proposals for a unified system of nomenclature of hepatitis C virus genotypes. Hepatology 42:962–973.

Suppiah V, Moldovan M, Ahlenstiel G, Berg T, Weltman M, Abate ML, Bassendine M, Spengler U, Dore GJ, Powell E, Riordan S, Sheridan D, Smedile A, Fragomeli V, Müller T, Bahlo M, Stewart GJ, Booth DR, George J. 2009. IL28B is associated with response to chronic hepatitis C interferon-alpha and ribavirin therapy. Nat Genet 41:1100–1104.

Tachi Y, Katano Y, Honda T, Hayashi K, Ishigami M, Itoh A, Hirooka Y, Nakano I, Samejima Y, Goto H. 2010. Impact of amino acid substitutions in the hepatitis C virus genotype 1b core region on liver steatosis and hepatic oxidative stress in patients with chronic hepatitis C. Liver Int 30:554–559.

Tanaka Y, Nishida N, Sugiyama M, Kurosaki M, Matsuura K, Sakamoto N, Nakagawa M, Korenaga M, Hino K, Hige S, Ito Y, Mita E, Tanaka E, Mochida S, Murawaki Y, Honda M, Sakai A, Hiasa Y, Nishiguchi S, Koike A, Sakaida I, Imamura M, Ito K, Yano K, Masaki N, Sugauchi F, Izumi N, Tokunaga K, Mizokami M. 2009. Genome-wide association of IL28B with response to pegylated interferon-alpha and ribavirin therapy for chronic hepatitis C. Nat Genet 41:1105–1109.

Thomas DL, Thio CL, Martin MP, Qi Y, Ge D, O'Huigin C, Kidd J, Kidd K, Khakoo SI, Alexander G, Goedert JJ, Kirk GD, Donfield SM, Rosen HR, Tobler LH, Busch MP, McHutchison JG, Goldstein DB, Carrington M. 2009. Genetic variation in IL28B and spontaneous clearance of hepatitis C virus. Nature 461:798–801.

Toyoda H, Kumada T, Tada T, Arakawa T, Hayashi K, Honda T, Katano Y, Goto H. 2010. Association between HCV amino acid substitutions and outcome of peginterferon and ribavirin combination therapy in HCV genotype 1b and high viral load. J Gastroenterol Hepatol 25:1072–1078.

Yahoo N, Sabahi F, Shahzamani K, Malboobi MA, Jabbari H, Sharifi H, Mousavi-Fard SH, Merat S. 2011. Mutations in the E2 and NS5A regions in patients infected with hepatitis C virus genotype 1a and their correlation with response to treatment. J Med Virol 83:1332–1337.

Yokozaki S, Katano Y, Hayashi K, Ishigami M, Itoh A, Hirooka Y, Nakano I, Goto H. 2011. Mutations in two PKR-binding domains in chronic hepatitis C of genotype 3a and correlation with viral loads and interferon responsiveness. J Med Virol 83:1727–1732.

Zeuzem S, Lee JH, Roth WK. 1997. Mutations in the nonstructural 5A gene of European hepatitis C virus isolates and response to interferon alfa. Hepatology 25:740–744.

IJC
International Journal of Cancer

# Comparative analyses of regulatory T cell subsets in patients with hepatocellular carcinoma: A crucial role of $CD25^{-}FOXP3^{-}$ T cells

Naruyasu Kakita[1], Tatsuya Kanto[1,2], Ichiyo Itose[3], Shoko Kuroda[1], Michiyo Inoue[1], Tokuhiro Matsubara[1], Koyo Higashitani[1], Masanori Miyazaki[1], Mitsuru Sakakibara[1], Naoki Hiramatsu[1], Tetsuo Takehara[1], Akinori Kasahara[4] and Norio Hayashi[3]

[1] Department of Gastroenterology and Hepatology, Osaka University Graduate School of Medicine, Suita, Japan
[2] Department of Dendritic cell Biology and Clinical Applications, Osaka University Graduate School of Medicine, Suita, Japan
[3] Kansai Rosai Hospital, Amagasaki, Japan
[4] Department of General Medicine, Osaka University Hospital, Suita, Japan

**Regulatory T cells (Tregs) play pivotal role in cancer-induced immunoediting. Increment of $CD25^{high+}FOXP3^{+}$ natural Tregs has been reported in patients with hepatocellular carcinoma (HCC); however, the involvement of other type of Tregs remain elusive. We aimed to clarify whether $FOXP3^{-}$ Tregs are increased and functionally suppressive or not in patients with HCC. We enrolled 184 hepatitis C-infected patients with chronic liver diseases or HCC, 57 healthy subjects and 27 HCC patients with other etiology. Distinct Treg subsets were phenotypically identified by the expression of CD4, CD25, CD127 and forkhead/winged helix transcription factor (FOXP3). Their gene profiles, frequency and suppressor functions against T cell proliferation were compared among the subjects. To examine the molecules involving in Treg differentiation, we cultured naive $CD4^{+}$ T cells in the presence of HCC cells and dendritic cells. We determined two types of $CD4^{+}CD127^{-}$ T cells with comparable regulatory ability; one is $CD25^{high+}$ cells expressing FOXP3 ($CD25^{high+}FOXP3^{+}$ Tregs) and the other is $CD25^{-}$ cells without $FOXP3^{-}$ expression ($CD25^{-}FOXP3^{-}$ cells). The peripheral or intrahepatic frequency of $CD25^{-}FOXP3^{-}$ Tregs in HCC patients is higher than those in other groups, of which significance is more than $CD25^{high+}FOXP3^{+}$ cells. Of importance, $CD25^{-}FOXP3^{-}$ Tregs, but not $CD25^{high+}FOXP3^{+}$ cells, dynamically change in patients accompanied by the ablation or the recurrence of HCC. $CD25^{-}FOXP3^{-}$ T cells with $CD127^{-}IL\text{-}10^{+}$ phenotype are inducible *in vitro* from naive $CD4^{+}$ T cells, in which programmed cell death 1 ligand 1, immunoglobulin-like transcript 4 and human leukocyte antigen G are involved.. In conclusion, $CD25^{-}FOXP3^{-}$ Tregs with suppressive capacity are increased in patients with HCC, suggesting their distinct roles from $CD25^{+}FOXP3^{+}$ Tregs.**

Hepatocellular carcinoma (HCC) is the fifth most common cancer and the third leading cause of cancer-related deaths in the world.[1] One of the most prevalent risk factors for HCC is hepatotropic viruses, such as hepatitis B (HBV) or C (HCV) virus.[2,3] In the process of HCC development, the involvement of tumor-induced immune suppression; *i.e.*, immunoediting, has been implicated. Regulatory T cells (Tregs) are unique subset of T cells, playing essential roles in the maintenance of immune homeostasis or in the protection of hosts from virulent infections and cancers.[4] Generally, the existence of two types of Tregs has been reported. One is naturally occurring $CD4^{+}CD25^{high+}$ Tregs, which are derived from the thymus and suppress auto-reactive T cells. The other is inducible or adaptive Tregs, including interleukin (IL)-10-secreting type-1 regulatory T cells (Tr1) and transforming growth factor (TGF)-β-producing Th3. These are inducible in the

**Key words:** HCC, regulatory T cells, FOXP3, CD25, CD127

**Abbreviations:** CTLA-4: cytotoxic T-lymphocyte antigen 4; DC: dendritic cell; FOXP3: forkhead/winged helix transcription factor; GITR: glucocorticoid-induced TNF receptor family-regulated gene; HBV: hepatitis B virus; HCC: hepatocellular carcinoma; HCV: hepatitis C virus; IL-T4: immunoglobulin-like transcript 4; LAG-3: lymphocyte-activation gene 3; PBMC: peripheral blood mononuclear cell; PD-1: programmed cell death 1; PD-L1: programmed cell death 1 ligand 1; RFA: radiofrequency ablation; RT-PCR: reverse transcription polymerase chain reaction; Tr1: type-1 regulatory T cells; Tregs: regulatory T cells

Additional Supporting Information may be found in the online version of this article.

**Grant sponsors:** Grant-In-Aid for Scientific Research from the Ministry of Education, Culture, Sports, Science and Technology of Japan, a Grant-in-Aid from the Ministry of Health, Labour and Welfare of Japan

**DOI:** 10.1002/ijc.27535

**History:** Received 23 Jul 2011; Accepted 28 Feb 2012; Online 15 Mar 2012

**Correspondence to:** Tatsuya Kanto, Department of Gastroenterology and Hepatology, Osaka University Graduate School of Medicine, 2-2 Yamadaoka, Suita 565-0871 Japan, Tel: +81-6-6879-3621, Fax: +81-6-6879-3629, E-mail: kantot@gh.med.osaka-u.ac.jp

Table 1. Clinical backgrounds of the patients enrolled in the study[1]

| | HV | CH (C) | LC (C) | HCC (C) | HCC (B) | HCC (NBNC) |
|---|---|---|---|---|---|---|
| N | 57 | 66 | 39 | 79 | 12 | 15 |
| Gender (M/F) | 35/22 | 44/22 | 23/16 | 44/35 | 8/4 | 9/6 |
| Age (years) | 56 ± 11 | 56 ± 18 | 61 ± 9 | 66 ± 11 | 56 ± 9 | 62 ± 13 |
| ALT (IU/l) | ND | 70 ± 15 | 44 ± 13 | 56 ± 17 | 65 ± 7 | 45 ± 11 |
| Platelets ($10^4/\mu l$) | ND | 15 ± 4 | 11 ± 4 | 12 ± 4 | 13 ± 4 | 12 ± 4 |
| Total bilirubin (mg/ml) | ND | 0.9 ± 0.4 | 1.6 ± 0.4[2] | 0.9 ± 0.3 | 0.6 ± 0.1 | 0.7 ± 0.3 |
| Alb (g/dl) | ND | 3.7 ± 0.5 | 3.3 ± 0.4 | 3.1 ± 0.6[2] | 3.5 ± 0.2 | 3.6 ± 0.3 |
| AFP (ng/ml)[3] | ND | 2-115 (15) | 2-347 (16) | 4-33357 (43) | 7-12 (10) | 10-16520 (23) |
| TNM stage[4] (I + II/III + IV) | – | – | – | 55/24 | 9/3 | 9/6 |

[1]All values except for AFP are expressed as mean ± standard deviation. [2]$p < 0.05$ *vs.* CH (C) group. [3]Values are expressed as range (median).
[4]Seventh edition of International Union Against Cancer TNM staging system of HCC.
Abbreviations: HV, healthy volunteers; CH (C), LC (C), HCC (C), HCV-positive chronic hepatitis, liver cirrhosis and hepatocellular carcinoma; HCC (B), HBV-positive hepatocellular carcinoma; HCC (NBNC), non-B, non-C hepatocellular carcinoma; ALT, alanine aminotransferase; Alb, albumin; AFP, alfa-fetoprotein; ND, not determined.

periphery and are endowed with the ability to suppress antigen-specific T cells.[5] Several reports have shown that natural Tregs are increased in peripheral blood and/or tumor in patients with various types of cancer.[6] In HBV-infected HCC patients, an increase in natural Tregs and their suppressor functions against antigen-specific CTLs has been reported.[7] A correlation has been observed between natural Treg frequency and recurrence-free or overall survival of HCC patients.[8] However, it is yet to be determined if a distinct Treg subset is involved or not in the development of HCC.

The forkhead/winged helix transcription factor, FOXP3, is acknowledged as a major and specific marker of Tregs, the cellular expression of which is correlated with suppressive activities.[9] However, in the differentiation from naive T cells to effector/memory T cells, FOXP3 is transiently expressed but not sustained, suggesting that some proportion of $FOXP3^+$ T cells are not regulatory but activated ones.[10] These observations suggest that using FOXP3 as a marker of functionally regulatory cells would be limited and not suitable for adaptive Tregs. In recent studies, the expression of IL-7 receptor alpha chain (CD127) was found to be downregulated in Tregs and CD127 expression to be inversely correlated with FOXP3 expression.[11,12] Moreover, CD127-negative T cells are endowed with suppressive ability irrespective of their CD25 expression.[13] Alternatively, several studies have shown that CD127 is downregulated on $FOXP3^-$ Tr1 cells.[14,15] Due to the lack of specific or appropriate markers for identification of adaptive Tregs, it is yet to be confirmed that $FOXP3^-$ T cells are adaptive Tregs. Furthermore, little is known about the precise roles of $FOXP3^-$ regulatory cells in the development of HCC.

In this study, we focused on $FOXP3^-$ Tregs and tried to elucidate whether or not such cells are associated with the presence of HCC. To assess the feasibility of $FOXP3^-$ cells as a therapeutic target for immunological control of HCC, we tried to clarify the molecular mechanisms of its induction.

## Material and Methods

### Subjects

Among chronically HCV-infected patients who had been followed at Osaka University Hospital, we enrolled 184 patients who were further categorized into three groups according to the stages of liver disease: chronic hepatitis (CH), liver cirrhosis (LC) and HCC groups. The clinical stage of HCC was determined according to the TNM classification system of the International Union against Cancer (seventh edition). The study protocol was approved by the ethical committee at the Osaka University Graduate School of Medicine. At enrollment, written informed consent was obtained from all patients and volunteers. Some of HCC patients in this study received radiofrequency ablation (RFA) therapy. Indication for RFA therapy was based on therapeutic guidelines for HCC promoted by the Japan Society of Hepatology.[16] After the RFA session, the efficacy of tumor ablation or HCC recurrence thereafter was evaluated by computed tomography or magnetic resonance imaging scanning. In some of the HCC patients who underwent surgical resection, cancerous and adjacent noncancerous tissues were obtained at operation for further Treg analyses. As controls, 57 healthy subjects (HS) without history of liver diseases, 27 HCC patients with HBV infection (HBV–HCC group), those without HBV and HCV (non-B–, non-C [NBNC]–HCC group). The clinical backgrounds of the subjects are shown in Table 1.

### Frequency analyses of peripheral and liver-infiltrating Tregs

Peripheral blood mononuclear cells (PBMCs) were stained with a combination of various fluorescence-labeled anti-human mouse or rat monoclonal antibodies (mAbs) as reported previously (17). The mAbs for CD4, CD25, CD127, FOXP3 and IL-10 were purchased from Becton Dickinson Biosciences (San Jose, CA). Fresh liver specimens were

washed twice with phosphate-buffered saline and were diced into 0.5 mm pieces. After these pieces were passed through a nylon mesh, liver-infiltrating lymphocytes were isolated by Ficoll-Hypaque density gradient centrifugation. These cells were stained with fluorescence-labeled Abs as performed for PBMC. For the analyses of FOXP3 and IL-10, we performed intracellular staining using a human FOXP3 staining kit (BD Biosciences) according to the manufacturer's instructions. The stained cells from PBMC or liver were analyzed by FACS Canto (BD Biosciences) and Cell Quest software.

### Functional analysis of regulatory T cell subsets

To obtain live Tregs for functional analyses, we collected four populations of $CD4^+$ T cells according to the patterns of CD25 and CD127 expressions by FACS Aria (BD Biosciences). We cocultured various numbers of sorted cells with $1 \times 10^5$ allogenic naive $CD4^+CD25^-$ T cells in the presence of agonistic anti-CD3 and anti-CD28 Abs (BD Biosciences Pharmingen) on 96-well flat-bottom plates (Corning, Corning, NY) for 5 days. The proliferation of cells was assessed by incorporation of [3H]-thymidine. To clarify the suppression mechanism by Tregs, the cells were cultured with or without separation by transwell inserts (pore size 0.4 μm, Corning). Alternatively in some experiments, the cells were cultured in the presence or absence of neutralizing 10 ng/ml anti-IL-10 or anti-TGF-β Abs (R&D Systems, Mckinley, MN) or isotype IgG.

To examine regulatory cells possess suppressive function on recall antigen-specific $CD4^+$ T cell responses, we cocultured $1 \times 10^4$ each of sorted cells from some HCC patients with $1 \times 10^5$ autologous $CD4^+$ T cells in the presence or absence of 20 μg/ml of tetanus toxoid (Sigma) for 5 days, stimulated with 10 IU/ml of recombinant human IL-2 (BD Pharmingen). The proliferation of cells was assessed using WST-8 (2-(2-methoxy-4-nitrophenyl)-3-(4-nitrophenyl) -5 -(2,4-disulfophenyl)-2H-tetrazolium, monosodium salt) reagent in the Cell Counting Kit-8 (Dojindo, Japan) according to the manufacturer's instructions.

### Real-time RT-PCR

To analyze gene profiles of Tregs, we collected $CD4^+CD25^{high+}CD127^-$ and $CD4^+CD25^-CD127^-$ T cells using FACS Aria. Extraction of total RNA and subsequent real-time reverse transcription polymerase chain reaction (RT-PCR) was performed as reported previously with some modifications.[17] Assays-on-demand primers and probes (Applied Biosystems, Foster City, CA) were used to quantify FOXP3, cytotoxic T-lymphocyte antigen 4 (CTLA-4), glucocorticoid-induced TNF receptor family-regulated gene (GITR), lymphocyte-activation gene 3 (LAG3), IL-21, programmed cell death 1 (PD-1) and c-masculoaponeurotic fibrosarcoma (c-Maf) expression. The expressions of molecules were given as the relative values to the calibrator samples. To standardize the amount of total RNA, we quantified β-actin mRNA from each sample as a control of internal RNA and corrected all values with this.

### Induction of $CD4^+CD25^-CD127^-FOXP3^-$ T cells from PBMC

To clarify the molecular mechanisms of Treg induction, we cultured $1 \times 10^6$ naive $CD4^+CD25^-$T cells with $1 \times 10^5$ autologous monocyte-derived dendritic cells (DCs) and mitomycin C (Sigma-Aldrich, St. Louis, MO)-treated $1 \times 10^5$ HCC cell lines, Huh7 or HepG2 (AmericanType Culture Collection, Manassas, VA) on 24-well flat-bottom plates for 5 days. Monocyte-derived DCs were generated from $CD14^+$ cells as reported previously.[18] On days 2 and 4 of the coculture, recombinant human IL-2 (10 IU/ml), IL-10 (20 IU/ml) and IL-15 (20 IU/ml; BD Pharmingen) were added to the cells. On day 6, they were stimulated with phorbol 12-myristate 13 acetate (PMA; 1 ng/ml) and ionomycin (1 μmol/l) in the presence of anti-CD3 mAb (1 μg/ml) and breferdin A (1 μg/ml) (BD Pharmingen). In some experiments, we separated relevant cells by transwell inserts (pore size 0.4 μm) or added 10 μg/ml neutralizing Abs against TGF-β (R&D), HLA-DR (BD), PD-1 (R&D), programmed cell death 1 ligand 1 (PD-L1; e-Bioscience) or immunoglobulin-like transcript 4 (IL-T4) (e-Bioscience) during the culture. Subsequently, the cells were stained with Abs for CD4, CD25, CD127, FOXP3 and IL-10 and then were subjected to FACS analysis.

### Knockdown of PD-L1 and HLA-G genes in HCC cell lines by siRNA

To confirm the molecules involving Treg induction, we knocked down PD-L1 and HLA-G genes in Huh7 cells by means of RNA interference. We used the small interfering RNA (siRNA) cocktail targeting human CD274 (PD-L1) or human leukocyte antigen G (HLA-G), provided by COSMO BIO (Tokyo, Japan). Transfection of siRNA to Huh7 or HepG2 cells was performed using lipofectamine RNAiMAX (Invitrogen) according to the manufacturer's instructions. To assess the efficiency of transfection, we compared the mRNA expression of target genes before and after the procedure by real time RT-PCR.

### Statistical analyses

The Jonckheere-Terpstra test was used for the analysis of dose-dependent tendency. The Mann-Whitney nonparametric *U* test was used to compare differences in unpaired samples and Kruskal–Wallis nonparametric tests were used to compare differences among multiple groups, respectively. Friedman test with Bonferroni multiple comparison tests was used to compare differences in paired samples. All tests were two-tailed, and a $p < 0.05$ was considered statistically significant.

## Results

### $CD4^+$ T cells with distinct patterns of CD127 and FOXP3 expression were identified

According to the expression of CD25 and CD127 in $CD4^+$ T cells, we separated them into four groups: $CD25^{high+}CD127^-$, $CD25^-CD127^-$, $CD25^{high+}CD127^+$ and $CD25^-CD127^+$ cells, respectively (Fig. 1*a*). Most of the $CD4^+CD25^{high+}CD127^-$

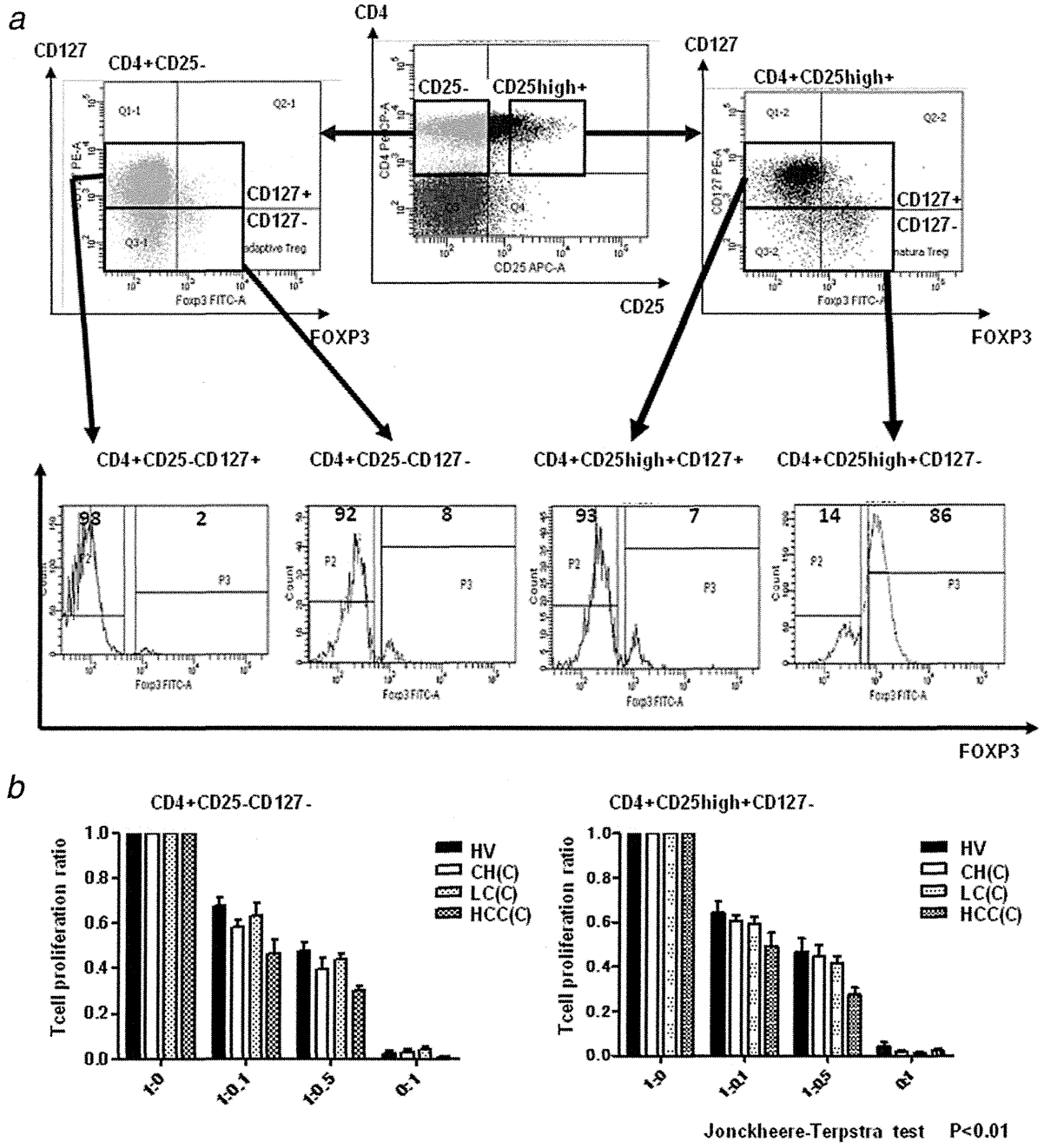


Figure 1. $CD4^+CD25^-CD127^-$ and $CD4^+CD25^{high+}CD127^-$ T cells are Tregs. (*a*) $CD4^+$ T cells are separated into four subpopulations: $CD4^+CD25^{high+}CD127^+$, $CD4^+CD25^{high+}CD127^-$, $CD4^+CD25^-CD127^+$ and $CD4^+CD25^-CD127^-$ cells, respectively. These cells were examined for FOXP3 expression. The numbers in the histograms depict the percentages of gated cells. Representative plots from three patients and donors are shown. (*b*) Sorted $CD4^+CD25^-CD127^-$ T cells and $CD4^+CD25^{high+}CD127^-$ T cells obtained from patients and healthy donors were added at various ratios to allogenic $CD4^+$ T cells stimulated with anti-CD3 and anti-CD28 Abs. After 5 days of culture, $CD4^+$ T cell proliferation was evaluated by incorporation of $^3$H-thymidine. The bars indicate the ratio of counts per minutes (cpm) in various responders to regulatory cells ratio to those at 1:0. The results are shown as mean + SEM of ten patients or donors in each group. The dose dependency was analyzed by Jonckheere Terpstra test and comparison among the disease statuses was analyzed by Wilcoxon rank sum test with Bonferroni multiple comparison test. HV, healthy volunteers; CH(C), LC(C), HCC (C), HCV-infected chronic hepatitis, liver cirrhosis or hepatocellular carcinoma, respectively.

cells express FOXP3 (>80%). In contrast, the populations of $CD4^+CD25^-CD127^-$, $CD4^+CD25^{high+}CD127^+$ and $CD4^+CD25^-CD127^+$ lack FOXP3 expression (<10%). These results show that, except for $CD4^+CD25^{high+}CD127^-$ cells, the remaining $CD127^-$ cells lack FOXP3 and CD25 expression ($CD4^+CD25^-CD127^-FOXP3^-$).

### $CD4^+CD25^{high+}CD127^-$ cells and $CD4^+CD25^-CD127^-$ T cells are suppressors against allogeneic T cells with distinct mechanisms

To examine which cell populations exert a suppressive capacity, we added each phenotype of cells separated from the subjects to allogeneic $CD4^+$ T cells. The sorted $CD4^+CD127^+$ T cells had no regulatory activities regardless of CD25 expression (data not shown). In contrast, $CD127^-$ cells, either $CD25^-$ or $CD25^{high+}$, significantly inhibited allogenic $CD4^+$ T cell proliferation in a dose-dependent manner, at comparable levels (Fig. 1*b*). Of note is that their suppressive capacity did not differ at the single cell level between patients and donors, regardless of the stage of liver disease (Fig. 1*b*). In addition, $CD127^-$ cells are anergic irrespective of CD25 expression (Fig. 1*b*). The suppressive ability of $CD4^+CD25^{high+}CD127^-$ cells was significantly abrogated by transwells and anti-TGF-β Ab, suggesting that they work in cell–cell contact-dependent and TGF-β-dependent manners (Supporting Information Fig. 1). By contrast, suppression by $CD4^+CD25^-CD127^-$ cells was alleviated by anti-IL-10 Ab but not by transwells, showing that they are contact-independent but IL-10-dependent (Supporting Information Fig. 1). These results show that $CD4^+CD25^-CD127^-$ cells possess a suppressive capacity with distinct machinery from $CD4^+CD25^{high+}CD127^-$ cells. In the setting of tetanus toxoid-reactive $CD4^+$ T cell response, each type of cells tended to be comparably suppressive (Supporting Information Fig. 2).

### $CD4^+CD25^{high+}CD127^-$ and $CD4^+CD25^-CD127^-$ T cells display distinct gene profiles

$CD4^+CD25^{high+}CD127^-$ and $CD4^+CD25^-CD127^-$ T cells were sorted by FACS Aria and were subjected to real-time RT-PCR analyses. The expressions of FOXP3, CTLA-4 and GITR in $CD4^+CD25^{high+}CD127^-$ cells were higher than those in $CD4^+CD25^-CD127^-$ T cells, while those of LAG-3, IL-21, PD-1 and c-Maf in $CD4^+CD25^-CD127^-$ T cells were higher than those in $CD4^+CD25^{high+}CD127^-$ cells, respectively (Fig. 2). Thus, these two types of regulatory cells have distinct molecular profiles. As we described in the previous sections, $CD4^+CD25^-CD127^-$ cells with regulatory capacity lack FOXP3 expression (Figs. 1 and 2). Thus, we tentatively defined such cells as $CD25^-FOXP3^-$ Tregs in the following parts.

### $CD25^-FOXP3^-$ Tregs are increased in HCC patients and their increments are associated with cancer progression

We compared the frequency of Treg subsets among healthy donors and HCV-infected patients. In HCC patients, $CD25^-FOXP3^-$ Tregs or $CD4^+$ $CD127^-$ $CD25^{high+}$ $FOXP3^+$ cells ($CD25^{high+}FOXP3^+$ Tregs) frequency in the periphery was significantly higher than those in other groups (Fig. 3*a*). The frequency of each type of Tregs is not correlated with HCV quantity (Supporting Information Fig. 3). These results show that the increase in $CD25^-FOXP3^-$ or $CD25^{high+}FOXP3^+$ Tregs is correlated with the development of liver cancer, but not with HCVRNA titers. Such increment of peripheral Tregs is also observed in HBV-HCC or NBNC-HCC patients (Fig. 3*a*).

Next, we compared the frequency of Tregs between PBMC and liver-infiltrating lymphocytes in HCC patients. Both $CD25^-FOXP3^-$ and $CD25^{high+}FOXP3^+$ Tregs are detected in liver-infiltrating lymphocytes, and $CD25^-FOXP3^-$ Tregs are higher in tumor-infiltrating lymphocytes than those in nontumor-infiltrating and circulating lymphocytes (Fig. 3*b*). These results demonstrate that $CD25^-FOXP3^-$ Tregs increase both in the liver and in the periphery in parallel with the development of cancer.

We serially examined the frequency of $CD25^-FOXP3^-$ Tregs and $CD25^{high+}FOXP3^+$ Tregs before and after RFA therapy. The $CD25^-FOXP3^-$ Tregs frequency dramatically decreased after successful HCC ablation and further subsided in patients without intrahepatic recurrence (Fig. 4*a*). In clear contrast, in patients with subsequent HCC recurrence, $CD25^-FOXP3^-$ Tregs increased before apparent radiological identification of HCC (Fig. 4*a*). Such dynamic frequency changes in parallel with HCC recurrence were not apparent in $CD25^{high+}FOXP3^+$ Tregs (Fig. 4*b*). Therefore, $CD25^-FOXP3^-$ Treg frequency is more closely correlated than $CD25^{high+}FOXP3^+$ Tregs with the presence or absence of HCC.

### PD-L1, IL-T4 and HLA-G are involved in the induction of $CD4^+CD25^-CD127^-FOXP3^-$ $IL\text{-}10^+$ T cells

After the culture of naive $CD4^+$ T cells, DC and Huh7 or HepG2, we found that $CD4^+CD25^-CD127^-FOXP3^-$ cells produce IL-10 (Fig. 5*a*), whereas $CD4^+CD25^+CD127^-FOXP3^+$ cells do not (Supporting Information Fig. 4). Since $CD4^+CD25^-CD127^-$ cells use IL-10 as one of suppressor mechanisms (Supporting Information Fig. 1), such $IL\text{-}10^+$ $CD4^+CD25^-CD127^-FOXP3^-$ T cells are functionally competent $CD25^-FOXP3^-$ Tregs (Fig. 5*a*). In culture, the frequency of $IL10^+$ $CD25^-FOXP3^-$ T cells decrease in the presence of anti-TGF-β, anti-PD-1, anti-PD-L1 or anti-ILT4 Abs, with the difference being the most significant with anti-PD-L1 or anti-ILT4 Abs (Fig. 5*b*). Next, in the absence of DC or the separation of T cells from HCC cell lines significantly reduced $IL10^+$ $CD25^-FOXP3^-$ T cell induction, whereas separation of T cells from DC did not change it (Fig. 5*c*). These results indicate that the contact between T cells and HCC cell lines is indispensable for $IL\text{-}10^+$ $CD25^-FOXP3^-$ T cell induction, but the contacts between T cells and DC or between DC and HCC cell lines are not, respectively. Similarly, the addition of anti-PDL1 or anti-IL-T4 Abs to this culture resulted in suppression of $IL\text{-}10^+$ $CD25^-FOXP3^-$ T cell induction, regardless of the presence of transwells (Fig. 5*c*).

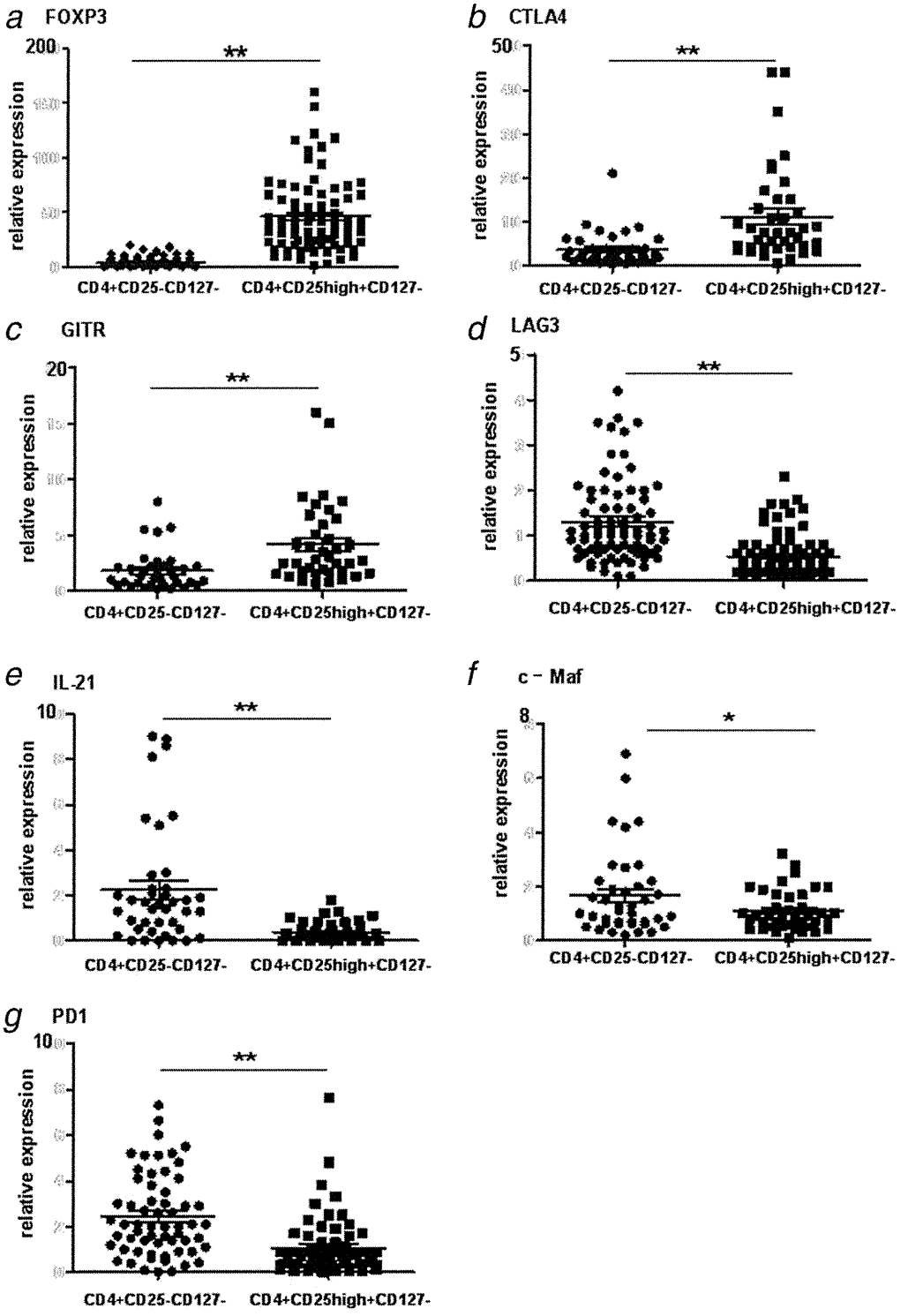


Figure 2. $CD4^+CD25^-CD127^-$ T cells and $CD4^+CD25^{high+}CD127^-$ T cells display distinct gene profiles. Sorted $CD4^+CD25^-CD127^-$ cells and $CD4^+CD25^{high+}CD127^-$ cells from PBMC of HCC patients were subjected to real-time RT-PCR for the analyses of FOXP3 (*a*), CTLA4 (*b*), GITR (*c*), LAG3 (*d*), IL-21 (*e*), c-Maf (*f*) and PD1 (*g*). The results are shown in relative expression of relevant genes to those of β-actin. *: $p < 0.05$; **: $p < 0.01$ by Mann-Whitney *U* test with Welch's correction.